Journal of Food and Drug Analysis

Volume 31 | Issue 4 Article 12

Isolation of GLP-1 enhancing indolizidine alkaloids from Boehmeria formosana

Recommended Citation
Lu, Ching-Yi; Huang, Zheng-Ying; Chen, Meng-Chin; Liu, Hui-Kang; Lee, Shoei-Sheng; and Chang, Chia-Chuan (2023) "Isolation of GLP-1 enhancing indolizidine alkaloids from Boehmeria formosana," *Journal of Food and Drug Analysis*: Vol. 31 : Iss. 4 , Article 12.
Available at: https://doi.org/10.38212/2224-6614.3483

Isolation of GLP-1 enhancing indolizidine alkaloids from *Boehmeria formosana*

Ching-Yi Lu [a], Zheng-Ying Huang [a], Meng-Chin Chen [a], Hui-Kang Liu [b], Shoei-Sheng Lee [a,**], Chia-Chuan Chang [a,*]

[a] School of Pharmacy, College of Medicine, National Taiwan University, Taipei 10050, Taiwan
[b] National Research Institute of Chinese Medicine, Taipei 11221, Taiwan

Abstract

***Boehmeria formosana*, with its related species, demonstrates anti-glycemic effect, inhibition of HBV production, anti-cancer activities, etc. Some indolizidine alkaloids from the same genus are bioactive but sensitive to light. To overcome this problem and obtain more phenanthroindolizidine alkaloids, isolation was performed in darkness, yielding 10 new indolizidine alkaloids and 17 known compounds. Among them, seven enhanced glucagon-like receptor 1 (GLP-1) activity at 50 mM, especially 14 and 6 (3.5- and 2.3-fold than the negative control). This procedure yielded bioactive indolizidine alkaloids with novel structures.**

Keywords: α-glucosidase inhibitor, *Boehmeria formosana,* GLP-1-enhancing ability, Phenanthroindolizidine alkaloids, Secondary metabolites

1. Introduction

Boehmeria formosana Hayata, (Urticacea) is one of the native *Boehmeria* species in Taiwan. There are about 120 species of *Boehmeria* worldwide, mainly in tropical and subtropical regions, and 10 species in Taiwan. The reported bioactivities of *Boehmeria* species include antioxidant [1], anti-hepatitis B [2—4], anti-diabetes [5], cell cytotoxic [6], and other activities. The active compounds in *Boehmeria* species include triterpenoids and steroids [6—9], alkaloids [6,10,11], chromone derivatives [5,7,8,12,13], anthraquinones [8] and phenylpropanoids [7].

According to the World Health Organization (WHO), diabetes mellitus (DM) is in the top 10 causes of death [14]. In addition to insulin supplements, several types of oral antidiabetic drugs are currently available, such as sulfonylureas, α-glucosidase inhibitors and thiazolidinediones. However, these drugs have side effects, such as gastrointestinal discomfort, weight gain and hypoglycemia [15].

In addition to the above treatment methods, promoting the secretion of glucagon-like peptide 1 (GLP-1) is a new treatment strategy for type 2 diabetes. GLP-1 is an incretin peptide and intestinal hormone produced by L cells in the ascending colon and distal ileum [16] to stimulate the beta cells in the pancreas to secrete insulin. In addition to acting on the pancreas, GLP-1 also acts on the hypothalamus and the stomach to directly reduce appetite [17] and delay stomach emptying, respectively [18]. When GLP-1 is secreted into the blood, it is immediately decomposed by dipeptidyl peptidase 4 (DPP-4). Such properties and roles of GLP-1 and DPP-4 led to the development of GLP-1 analogs and DPP-4 inhibitors for the treatment of type 2 DM [19].

Bioactivities of the *Boehmeria* genus are related to indolizidine alkaloids, of which some are sensitive to light. For example, dissolving indolizidine alkaloids in $CHCl_3$ under the bright ambient lighting condition yielded isoquinolinum salts, which were high polar substances that could cause a severe tailing effect in the normal phase silica gel chromatography. When the isolation work for such compounds is performed in darkness, more sensitive compounds are retained. To obtain more phenanthroindolizidine alkaloids, the isolation work is

Received 7 June 2023; accepted 7 November 2023.
Available online 15 December 2023

* Corresponding author. Fax: +886-2-23919098.
** Corresponding author. Fax: +886-2-23916127.
E-mail addresses: shoeilee@ntu.edu.tw (S.-S. Lee), chiachang@ntu.edu.tw (C.-C. Chang).

https://doi.org/10.38212/2224-6614.3483

conducted in the dark condition without ambient lighting [20–22]. The present study compared the differences of phenanthroindolizidine alkaloids obtained from the *n*-BuOH soluble fraction of *B. formosana* EtOH extract under the bright or dark conditions, followed by evaluation of their GLP-1 secretion enhancing ability.

2. Experimental

2.1. General

Instruments to obtain physical data for the compounds were as follows. NMR: a Bruker DPX-200 (200 MHz), AV-400 (400 MHz), AVIII-600 (600 MHz) or AVIII-800 (800 MHz) NMR (Rheinstetten, Germany) with a dual CryoProbe, *J* in Hz, δ in ppm calibrated by δ_H 3.30/δ_C 49.0 for CD_3OD, the 2D NMR spectra acquired by standard pulse sequences; ESI-MS: an Esquire 2000 ion trap mass spectrometer (Bruker Daltonics, Germany); thin-layer chromatography (TLC): silica gel 60 F_{254} aluminum sheets (0.25 mm) (Merck KGaA, Germany); column chromatography: Sephadex LH-20 (Pharmacia Fine Chemicals, Inc., USA) and Lobar, Lichrospher RP-18 (size B; 40–63 μm, 310 × 25 mm) (Merck); centrifugal partition chromatography (CPC): model L.L.B-M (230 mL; Sanki Engineering Limited, Japan); high performance liquid chromatography (HPLC): a Hitachi HPLC (Tokyo, Japan) equipped with a D-7000 interface, L-7100 pump, and an L-7400 UV-VIS or an L-7455 diode array detector; HPLC columns: Phenomenex Prodigy ODS (3) 100A columns (5 μm; 250 × 4.6 mm for analysis or 250 × 10 mm for semi-preparation) (Torrance, CA, USA).

2.2. Material

B. formosana Hayata used in this study were collected in Fushan Botanical Garden, Yilan, Taiwan, on September 20, 2017. The plant was identified by Prof. Shoei-Sheng Lee and Mr. Wan-Bao Chen (Fushan Botanical Garden, Yilan, Taiwan). The voucher specimen (No. 4638P) was deposited in the School of Pharmacy of the same university.

2.3. Extraction and isolation

2.3.1. Isolation of n-BuOH soluble fraction from B. Formosana leaf EtOH extract in the bright condition

According to TLC with Dragendorff's reagent, the *n*-BuOH soluble layer from the EtOH extract of the *B. formosana* leaves was rich in alkaloids. The *n*-BuOH soluble fraction from the EtOH extract of *B. formosana* leaves (10.4 g) was dissolved in an adequate volume of MeOH and fractionated with a Sephadex LH-20 column (100% MeOH) to give 10 subfractions. Fr. 5 (3.3 g) was isolated via silica gel chromatography ($CHCl_3$: MeOH = 9:1). Fr. 5-1 (119.5 mg) was isolated with Lobar A [0.1% MeOH: TFA = 9:11–11:9, 2.5 mL/min], **7** (21.7 mg) were collected from this fraction. Fr. 6. (2.42 g) was also isolated with silica gel ($CHCl_3$: MeOH = 9:1). Fr. 6-4 was isolated with semi-preparative RP-18 HPLC (MeOH-0.1% TFA = 45:55–55:45, 2.2 mL/min, monitoring at UV 254, 280, 465 nm), **8** (19.4 mg, t_R 21 min) and **10** (9.7 mg, t_R 31 min) were successfully collected.

2.3.2. Isolation of n-BuOH soluble fraction from B. Formosana leaf EtOH extract in the dark condition

Experiments were repeated in the dark condition. MeOH soluble fraction of *n*-BuOH soluble layer from *B. formosana* leaf EtOH extract (17.3 g) was fractionated by a Sephadex LH-20 column to give 7 fractions. Fr. B-2 (7.8 g) was further fractionated with the same column to get Fr. B-2-2 (7.2 g), followed by isolated with a RP-18 column to get 5 subfractions.

Fr. B-2-2-1 (2.39 g) and Fr. B-2-2-3 (1.7 g) were subjected to repeated RP-18 and silica gel column chromatography to give **21** (195.9 mg) (Fr. B-2-2-1), **16** (2.1 mg) (from Fr. B-2-2-3), and **1** (8.0 mg) (from Fr. B-2-2-3). Fr. B-2-2-3-4 (1.16 g) was isolated with silica gel column chromatography [$CHCl_3$: MeOH-0.1% NH_4OH = 100:0–0:100] to obtain 7 subfractions. The second fraction (Fr. B-2-2-3-4-2) (163.1 mg) was subjected to repeated RP-18 column chromatography to get **20** (20.6 mg), **2** (13.7 mg, **15** (42.9 mg), **18** and **19** (14.0 mg and 12.9 mg, respectively). Fr. B-3 (3.9 g) was isolated with a RP-18 column to get 7 subfractions. The third fraction (Fr. B-3-3) (57.3 mg) was subjected to repeated RP-18 column chromatography to get **6** (4.7 mg). The fourth fraction (Fr. B-3-4) (16.0 mg) was also further purified with RP-18 column chromatography to get **17** (2.9 mg).

The ^1H NMR and ^{13}C NMR data of compounds **1, 2, 6, 7, 8, 10** and **16–19** were listed in Tables 1–4. The detailed process and yield of the known compounds **3–5, 11–15**, and **25–32** are described in the Supplementary Data.

2.4. In vitro evaluation of GLP-1 enhancing ability

2.4.1. Method

Five μL anti-active GLP-1-d2, 5 μL anti-active GLP-1-$Tb3^+$ cryptate working solution with 10 μL samples were added into each well of 96-well plate,

*Table 1. ^{1}H and ^{13}C NMR data for **1** and **2**.*

Position	1[a]		2[b]	
	δ_H m (J/Hz)	δ_C	δ_H m (J/Hz)	δ_C
1	3.61 t (7.3)	23.2 (CH_2)	2.29–2.31 m	19.2 (CH_2)
2	2.40 quin (7.3)	23.1 (CH_2)	2.32–2.34 m 2.04–2.08 m	25.9 (CH_2)
3	4.80 t (7.3)	60.7 (CH_2)	3.96–3.97 m 3.76–3.78 m	66.5 (CH_2)
5	8.44 d (8.1)	145.3 (CH)	3.97–3.99 m 3.87 t (12.1)	66.5 (CH_2)
6	7.90 d (8.1)	128.2 (CH)	3.57 td (12.1, 4.2)	43.6 (CH)
7	–	152.8 (C)	3.10 ddd (13.2, 12.1, 4.2)	46.8 (CH)
8	–	138.0 (C)	2.34 m 2.18 br dt (13.2, 6.7, 3.2)	31.6 (CH_2)
9	–	158.2 (C)	3.97 m	75.7 (CH)
1′	–	125.5 (C)	–	130.0 (C)
2'/6′	–	–	7.06 d (8.6)	129.4 (CH)
3'/5′	–	–	6.76 d (8.6)	114.1 (CH)
2′	7.28 d (2.0)	113.3 (CH)	–	–
3′	–	151.0 (C)	–	–
4′	–	153.3 (C)	–	159.5 (C)
5′	7.20 d (8.9)	113.0 (CH)	–	–
6′	7.28 dd (8.9, 2.0)	123.7 (CH)	–	–
1″	–	128.1 (C)	–	134.7 (C)
2″	–	–	6.58 d (2.3)	111.9–112.0 (CH)
3″	–	–	–	149.2 (C)
4″	–	162.4 (C)	–	148.3 (C)
5″	–	–	6.74 d (8.2)	111.9–112.0 (CH)
6″	–	–	6.67 dd (8.2, 2.3)	120.0 (CH)
2"/6″	7.55 d (8.8)	131.2 (CH)	–	–
3"/5″	7.14 d (8.8)	115.8 (CH)	–	–
OMe-3′	3.91 s	56.6 (CH_3)	–	–
OMe-4′	3.93 s	56.8 (CH_3)	3.69 s	54.5–55.4 (CH_3)
OMe-3″	–	–	3.72 s	54.5–55.4 (CH_3)
OMe-4″	3.88 s	56.0 (CH_3)	3.67 s	54.5–55.4 (CH_3)

[a] Bruker AV-400 NMR spectrometer in methanol-d_4.
[b] Bruker AVIII-600 NMR spectrometer in methanol-d_4.

*Table 2. ^{1}H and ^{13}C NMR data for **7** and **8**.*

Position	7		8	
	δ_H m (J/Hz)[a]	δ_C[b]	δ_H m (J/Hz)[a]	δ_C[b]
1	3.67 t (7.7)	62.15 (CH_2)	3.56 t (7.6)	56.1 (CH_2)
2	2.53 quin (7.7)	22.9 (CH_2)	2.50 quin (7.6)	22.8 (CH_2)
3	4.97 t (7.7)	61.1 (CH_2)	5.09 t (7.6)	61.2 (CH_2)
5	9.13 d (1.4)	161.6 (CH)	9.23 s	137.5 (CH)
6	–	140.7 (C)	–	140.2 (C)
7	–	155.9 (C)	–	140.0 (C)
8	8.60 d (1.4)	142.3 (CH)	8.25 s	142.0 (CH)
9	–	155.6 (C)	–	155.3 (C)
1′	–	139.8 (C)	–	127.0 (C)
2'/6′	7.79 d (8.8)	129.8 (CH)	7.85 d (8.9)	129.8 (CH)
3'/5′	7.13 d (8.8)	116.2 (CH)	7.15 d (8.9)	116.2 (CH)
4′	–	162.9 (C)	–	162.7 (C)
1″	–	128.1 (C)	–	126.7 (C)
2"/6″	7.58 d (8.8)	131.2 (CH)	7.56 d (8.7)	131.4 (CH)
3"/5″	7.12 d (8.8)	115.8 (CH)	7.01 d (8.7)	115.8 (CH)
4″	–	162.5 (C)	–	160.2 (CH)
3-OMe	3.87 s	54.6	–	–
6-OMe	3.86 s	55.9	–	56.4

[a] Bruker AVIII-600 NMR spectrometer in methanol-d_4.
[b] Observed in HSQC and HMBC.

*Table 3. ^{1}H and ^{13}C NMR data for **6** and **10**.*

Position	6		10	
	δ_H m (J/Hz)[a]	δ_C[b]	δ_H m (J/Hz)[a]	δ_C[b]
1	7.82 s	117.8 (CH)	7.63 d (9.0)	131.8 (CH)
2	–	152.0 (C)	7.40 dd (9.0, 2.5)	115.5 (CH)
3	–	152.2 (C)	–	–
4	8.18 s	107.4 (CH)	9.30 d (2.5)	112.5 (CH)
4a	–	121.5 (CH)	–	–
4b	–	120.4 (CH)	–	–
5	8.14 d (1.4)	117.8 (CH)	–	–
6	–	162.7 (C)	–	–
7	7.44 dd (9.3, 1.6)	107.6 (CH)	8.73 d (9.1)	125.3 (CH)
8	8.36 d (9.1)	133.4 (CH)	8.66 d (9.1)	123.9 (CH)
8a	–	126.6 (C)	–	–
8b	–	138.7 (C)	–	–
9	10.08 s	140.9 (CH)	10.06 s	141.8 (CH)
11	4.55–4.58 m 4.22–4.23 m	59.8 (CH_2)	4.97 t (7.7)	59.7 (CH_2)
12	2.41–2.43 m 2.29–2.30 m	23.2 (CH_2)	2.61 quin (7.7)	22.8 (CH_2)
13	2.59–2.56 m	32.5 (CH_2)	3.63 t (7.7)	33.0 (CH_2)
13a	4.29–4.30 m	106.2 (CH)	–	–
14	5.76 d (4.0)	126.3 (CH)	8.99 s	114.0 (CH)
14a	–	155.1 (C)	–	–
14b	–	129.9 (C)	–	–
OMe-2/6	4.08–4.97 s	57.0	–	–
OMe-2	–	–	–	–
OMe-3	4.18 s	56.4	3.92 s	55.9
OMe-5	–	–	4.00 s	56.3
OMe-6	–	–	4.09 s	56.4

[a] Bruker AVIII-600 NMR spectrometer in methanol-d_4.
[b] Bruker AVIII-800 NMR spectrometer in methanol-d_4.

*Table 4. ^{1}H and ^{13}C NMR data for **16–19**.*

Position	16[a]		17		18		19	
	δ_H m (J/Hz)	δ_C	δ_H m (J/Hz)[a]	δ_C[c]	δ_H m (J/Hz)[b]	δ_C[c]	δ_H m (J/Hz)[a]	δ_C[c]
1	3.57 t (6.7)	33.4 (CH_2)	3.56 t (7.5)	33.3 (CH_2)	3.59 t (7.4)	33.4 (CH_2)	3.58 t (7.4)	33.4 (CH_2)
2	2.52 quin (6.7)	22.8 (CH_2)	2.52 quin (7.5)	22.8 (CH_2)	2.53 quin (7.4)	22.8 (CH_2)	2.53 quin (7.4)	22.9 (CH_2)
3	4.96 t (6.7)	61.1 (CH_2)	4.95 t (7.5)	61.1 (CH_2)	4.88 overlapped by CD_3OD	61.1 (CH_2)	4.87 overlapped by CD_3OD	61.1 (CH_2)
5	9.10 s	137.3 (CH)	9.06 s	137.1 (CH)	9.15 s	137.6 (CH)	9.17 s	137.9 (CH)
6	–	140.5 (C)	–	140.8 (C)	–	140.5 (C)	–	140.7 (C)
7	8.57 s	142.1 (CH)	8.54 s	141.9 (CH)	8.63 s	142.4 (CH)	8.63 s	142.5 (CH)
8	–	140.2 (C)	–	140.1 (C)	–	140.0 (C)	–	139.9 (C)
9	–	155.4 (C)	–	155.1 (C)	–	155.6 (C)	–	155.6 (C)
1′	–	127.0 (C)	–	126.9 (C)	–	127.0 (C)	–	127.5 (C)
4′	–	162.9 (C)	–	160.7 (C)	–	115.7 (C)	–	162.5 (C)
5′	–	–	–	–	–	–	7.15–7.13 m	113.5 (CH)
2′/6′	7.78 d (7.8)	129.8 (CH)	7.68 d (8.5)	129.8 (CH)	7.80 d (8.8)	129.8 (CH)	7.43–7.41 m	121.6 (CH)
3′/5′	7.12 d (7.8)	116.1 (CH)	6.97 d (8.5)	117.1 (CH)	7.15–7.11 m	116.1 (CH)	–	–
1″	–	126.8 (C)	–	125.8 (C)	–	128.6 (C)	–	128.1 (CH)
2″	–	–	–	–	7.21 d (2.3)	113.2 (CH)	–	–
3″	–	–	–	–	–	150.8 (C)	–	–
4″	–	160.4 (C)	–	160.2 (C)	–	151.8 (C)		152.5 (C)
5″	–	–	–	–	7.15–7.11 m	123.0 (CH)	–	–
6″	–	–	–	–	7.20 dd (8.7, 2.3)	113.1 (CH)	–	–
2″/6″	7.49 d (7.7)	131.2 (CH)	7.48 d (8.5)	131.2 (CH)	–	–	7.60 d (8.6)	131.3 (CH)
3″/5″	6.98 d (7.7)	117.1 (CH)	6.97 d (8.5)	117.5 (CH)	–	–	7.13 d (8.6)	115.7 (CH)
OMe-4′	3.87 s	56.0 (CH_3)	–	–	3.87 s	56.0 (CH_3)	3.90–3.88 s	56.0 (CH_3)
OMe-3′	–	–	–	–	–	–	3.90–3.88 s	56.6 (CH_3)
OMe-3″	–	–	–	–	3.90 s	56.6 (CH_3)	–	–
OMe-4″	–	–	–	–	3.90 s	56.8 (CH_3)	3.94 s	56.8 (CH_3)

[a] Bruker AVIII-600 NMR spectrometer in methanol-d_4.
[b] Bruker AV-400 NMR spectrometer in methanol-d_4.
[c] Bruker AVIII-800 NMR spectrometer in methanol-d_4.

and kept at rt for 1 d and analyzed with an ELISA reader. STC-1 cells were used as the target cell.

2.4.2. Data analysis

Signals of anti-active-d2 (acceptor) and anti-active GLP-1-Tb3^{+} cryptate (donor) in each well were calculated as follows.

$$\text{Ratio} = (\text{Signal 665 nm} / \text{Signal 620 nm}) \times 10^4$$

Then, delta F (%) was used to evaluate instrument accuracy and influence of background value.

$$\text{Delta F (\%)} = [(\text{Ratio sample} - \text{Ratio negative control}) / \text{Ratio negative control}] \times 100$$

3. Results

3.1. Isolation of secondary metabolites from B. Formosana

A total of 27 compounds were isolated in this study, and the chemical structures of these compounds are shown in Fig. 1. Among these compounds, **1**, **2**, **6**, **7**, **8**, **10** and **16**–**19** are newly described compounds. Furthermore, compound **1** is a compound with a new skeleton.

Isolation of the *n*-BuOH-soluble layer of *B. formosana* leaf EtOH extract in the bright condition gave an indolizidine (**4**), three secophenanthroindolizidines (**5**, **7** and **8**), three phenanthroindolizidines (**9**–**11**), a phenanthroquinolizidine (**28**), and a glycoside (**32**). To prevent the production of undesired isoquinolinum salts due to ambient light, isolation of the same layer was also performed in the dark condition, yielding 17 additional compounds, including three secophenanthroindolizidines (**1**–**3**), three phenanthroindolizidine alkaloids (**6** and **13**–**14**), five indolizidines (**15**–**19**), three cinnamaide alkaloids (**25**–**27**), and three glycosides (**29**–**31**). These results clearly indicate that the ambient light may affect stability of these compounds.

3.2. Structural elucidation of new compounds

3.2.1. Structural elucidation of diaryl indolizidines

3.2.1.1. Seco-formosanasine C (1). The molecular formula of **1** was determined as $C_{23}H_{24}NO_3$ by ESIMS and HR-ESIMS. The ^{1}H NMR spectrum showed an ABX system [δ_H 7.28 (d, J = 2.0 Hz, H-2′), δ_H 7.20 (d, J = 8.9 Hz, H-5′), δ_H 7.28 (dd, J = 8.9, 2.0 Hz, H-6′)], an AA'/BB′ system δ_H 7.55 (d, J = 8.8 Hz, H-2"/6″), δ_H 7.14 (d, J = 8.8 Hz, H-3"/5″)] and methoxy groups (δ_H 3.93, δ_H 3.91 and δ_H 3.88) (Table 1; Fig. S1). The *ortho*-coupling pattern of H-5 [δ 8.44 (d, J = 8.1 Hz)] and H-6 [δ 7.90 (d, J = 8.1 Hz)] did not match those of the reported skeletons of 6,7- and 6,8-diaryl-1,2,3,9-tetrahydroindolizidines, so it was identified as a novel 7,8-diaryl-1,2,3,9-tetrahydroindolizidine. Furthermore, δ 3.61 (t, J = 7.4 Hz, H-1), δ_H 2.40 (quin, J = 7.4 Hz, H-2) and δ_H 4.80 (t, J = 7.4 Hz, H-3) were considered as the signal on the nitrogen-contained five-membered heterocyclic ring. According to the NOESY spectrum (Fig. S5), the following correlations were observed: H-2'/OMe-3′, H-5'/OMe-4′, H-3"/OMe-4″, H-5"/H-6″, H-6"/H-1, H-6/H-2′, H-6/H-5, confirming the position of the methoxy groups and the moiety of 7,8-diaryl indolizidines. The ^{13}C NMR data also showed the characteristics of 7,8-diaryl tetrahydroindolizidine, including the signals of the two aryl groups at δ_C 152.8 and δ_C 138.0 and indolizine at δ_C 145.3 (C-5), δ_C 128.2 (C-6), δ_C 23.2 (C-1), δ_C 23.1 (C-2) and δ_C 60.7 (C-3). Therefore, the IUPAC name of **1** was determined to be 8-(4″-methoxyphenyl)-7-(3′,4′-dimethoxyphenyl)-1,2,3-trihydroindolizin-4-ium trifluoroacetate and it was named *seco*-formosanasine C.

3.2.1.2. 6,7-Diaryl indolizidines (2, 7 and 8). The molecular formula of **2** was determined as $C_{23}H_{29}NO_4$ by HR-ESIMS. The ^{1}H NMR spectrum of **2** also showed similar aryl signals of **1**: an ABX system [δ_H 6.67 (dd, J = 8.2, 2.3 Hz, H-6″), δ_H 6.74 (d, J = 8.2 Hz, H-5″), δ_H 6.58 (d, J = 2.3 Hz, H-2″)], an AA'/BB′ system [δ_H 7.06 (d, J = 8.8 Hz, H-2'/6′), δ_H 6.76 (d, J = 8.8 Hz, H-3'/5′)] and three aromatic methoxy groups (δ_H 3.72, δ_H 3.67, δ_H 3.69) (Table 1; Fig. S8). However, the two *ortho*-coupled aromatic signals were missing. The signals in the aliphatic region suggested it was a similar skeleton analog of desmethylsecoantofine *N*-oxide [23]. As shown in Fig. 2, compound **2** is proposed as a novel 6,7-diaryl-indolizine-*N*-oxide according to the similar ^{1}H and ^{13}C NMR spectra with those of desmethylsecoantofine *N*-oxide and 13a*R*-6-*O*-desmethylsecoantofine. This proposition is supported by the correlations observed in the 2D COSY (Fig. S11, H-5/H-6, H-6/H-7, H-7/H-8, H-8/H-9, H-9/H-1, H-1/H-2, H-2/H-3), NOESY (Fig. S13, H-6"/H-5″, H-5"/OMe-4″, H-6"/H-9, H-6"/H-8, H-6"/H-6, H-8/H-9, H-9/H-1, H-2'/H-6, H-2'/H-5) and HMBC (Fig. S12) spectra. The configuration for H-9 and *N*-oxide of **2** was *cis*, based on its chemical shift of H-9 (δ_H 3.97) in specific ranges of reported data (*cis*, 3.90–4.10 ppm; *trans*, 3.50–3.70 ppm) [22]. C-9 was identified as *S* form with the negative cotton effect at 279 nm in the circular dichroism (CD) spectrum (Fig. S15) [24,25]. In the NOESY spectrum, the correlations of H-6/H-7 and H-7/H-9 were observed, indicating that they

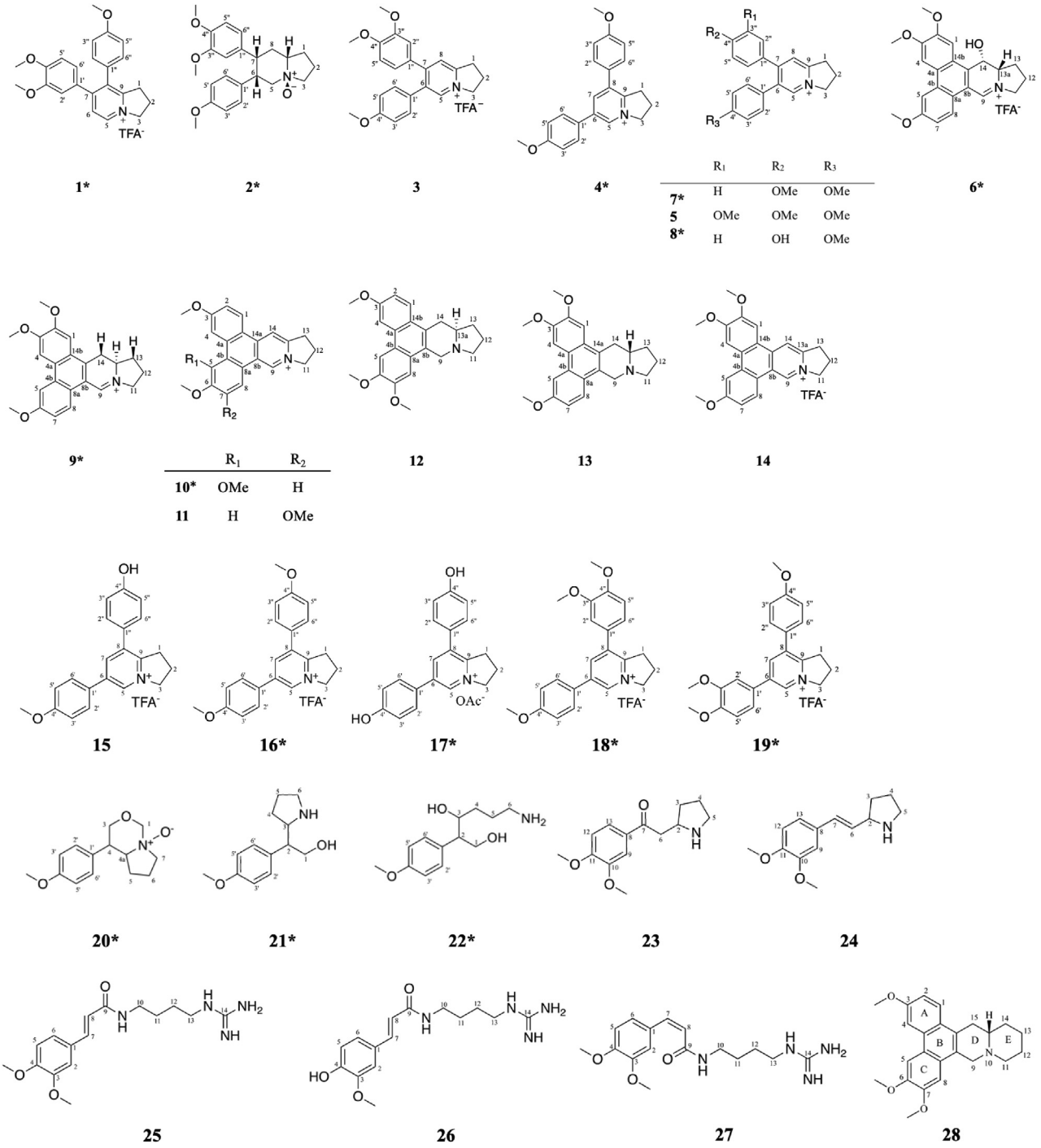

Fig. 1. Structures of compounds 1–32 from B. formosana.

had the same orientation. Therefore, compound **2** is a new compound, identified as (4*S*, 6*S*, 7*R*, 9*S*)-6-(4′-methoxyphenyl)-7-(3′,4′-dimethoxyphenyl)octahydro-indolizine-4-oxide.

The molecular formulae of **7** and **8** were determined as $C_{22}H_{22}NO_2$ and $C_{21}H_{20}NO_2$ by ESIMS and HR-ESIMS, respectively. The ^{1}H NMR data of both **7** and **8** (Table 2) had two AA'/BB′ systems (H-3"/H-5″, H-2"/H-6″, H-3'/H-5′, H-2'/H-6′). The sole methoxy signal at δ_H 3.87 and the molecular formula of **8** revealed the existence of a *para*-hydroxy group on another aromatic ring. Also, the NOESY spectrum (Fig. S32) confirmed the correlations of H-2'/H-5 and H-8/H-2". The HMBC spectrum (Fig. S31) showed the correlations between H-5/C-1′, H-6'/C-4′, C-4'/OMe-4'. Therefore, **7** is identified as 4′,4″-

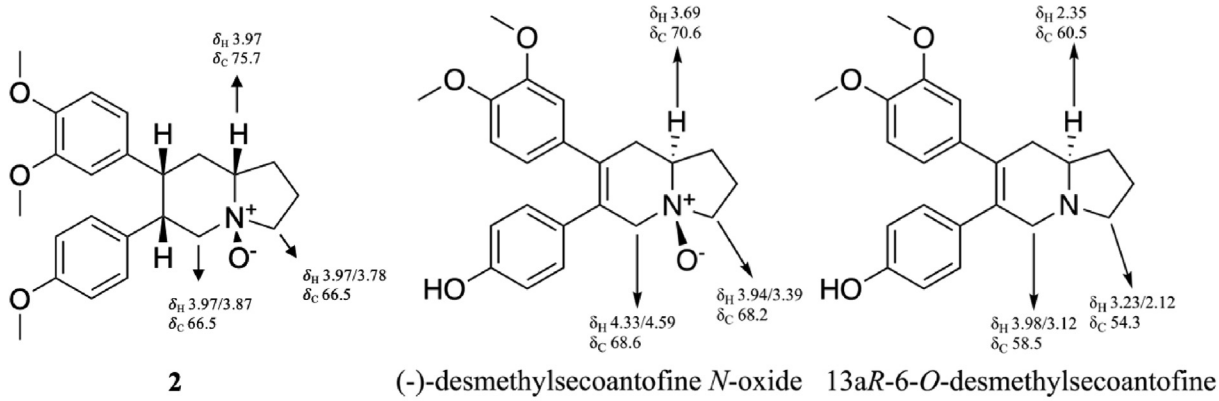

Fig. 2. Substituent effect of N-oxide on chemical shifts of secophenanthroindolizidine (^1H and ^{13}C NMR chemical shifts of (−)-desmethylsecoantofine N-oxide and 13aR-6-O-desmethylsecoantofine were measured in C_5D_5N on a 600 MHz NMR).

dimethoxy-6′,6″-*seco*-phenanthroindolizidine, with **8** as 4′-methoxy-4″-hydroxy-6′,6″-*seco*-phenanthroindolizidine and named *seco*-formosanasine A (**7**) and *seco*-formonsanasine B (**8**), respectively.

3.2.1.3. 6,8-Diaryl indolizidines (16–19). The molecular formulae of **16**–**19** were determined as $C_{21}H_{20}NO_2$, $C_{20}H_{18}NO_2$, $C_{23}H_{24}NO_3$ and $C_{23}H_{24}NO_3$ by HR-ESIMS, respectively. The ^1H and ^{13}C NMR spectra of **16**–**19** showed the characteristic signals for a 6,8-diaryl indolizidine (including the signals of two aryl groups at C-6 and C-8 and indolizine at C-1, C-2, C-3, C-5 and C-7), and were similar to the reported data of ficuseptine TFA salt (**15**) [23]. The ^1H NMR spectra of **16**–**19** showed the characteristic signals of 6,8-diarylindolizidinoids [**16**: δ_H 3.57 (t, J = 6.7 Hz, H-1), δ_H 2.52 (quin, J = 6.7 Hz, H-2), δ_H 4.96 (t, J = 6.7 Hz, H-3), δ_H 9.10 (s, H-5) and δ_H 8.57 (s, H-7); **17**: δ_H 3.56 (t, J = 7.6 Hz, H-1), δ_H 2.52 (quin, J = 7.6 Hz, H-2), δ_H 4.95 (t, J = 7.6 Hz, H-3), δ_H 9.06 (s, H-5) and δ_H 8.54 (s, H-7); **18**: δ_H 3.59 (t, J = 7.5 Hz, H-1), δ_H 2.53 (quin, J = 7.5 Hz, H-2), δ_H 4.88 (H-3), δ_H 9.15 (s, H-5) and δ_H 8.63 (s, H-7); **19**: δ_H 3.58 (t, J = 7.4 Hz, H-1), δ_H 2.53 (quin, J = 7.4 Hz, H-2), δ_H 4.87 (H-3), δ_H 9.17 (s, H-5) and δ_H 8.63 (s, H-7)]. Therefore, two AA′/BB′ systems [**16**: δ_H 7.49 (d, J = 7.7 Hz, H-6"/H-2″), δ_H 6.98 (d, J = 7.7 Hz, H-5"/H-3″) and δ_H 7.78 (d, J = 7.8 Hz, H-2′/H-6′), δ_H 7.12 (d, J = 7.8 Hz, H-3′/H-5′); **17**: δ_H 7.48 (d, J = 8.5 Hz, H-6"/H-2″), δ_H 6.97 (d, J = 8.5 Hz, H-5"/H-3″) and δ_H 7.68 (d, J = 8.5 Hz, H-2′/H-6′), δ_H 6.97 (d, J = 8.5 Hz, H-3′/H-5′)] were observed in the ^1H NMR spectra of **16** (Fig. S37) and **17** (Fig. S44). The ^1H NMR spectrum of **18** (Fig. S48) showed a set of 1,3,4-substituted aromatic ring signals [δ_H 7.21 (d, J = 2.3 Hz, H-2″), δ_H 7.20 (dd, J = 8.7, 2.3 Hz, H-6″) and δ_H 7.15–7.11 (m, H-5″)] and those of an AA′/BB′ system [δ_H 7.80 (d, J = 8.8 Hz, H-6′/H-2′), δ_H 7.15–7.11 (m, H-5′/H-3′)]. Furthermore, an AA′/BB′ system [δ_H 7.60 (d, J = 8.6 Hz, H-2"/H-6″) and δ_H 7.13 (d, J = 8.9 Hz, H-3"/H-5″)], an AMX system [δ_H 7.43–7.41 (m, H-6′/H-2′), δ_H 7.15–7.13 (m, H-5′)] appeared in the ^1H NMR spectrum of **19** (Table 4; Fig S53). The position of methoxy groups was confirmed by correlations in the NOESY spectra: **16** (Fig. S41): H-7/H-6′, H-6′/H-5′, H-5′/OMe-4′, H-5/H-6′, H-7/H-6″, H-6"/H-5″, H-6"/H-1; **17** (Fig. S46): H-7/H-6′, H-6′/H-5′, H-5/H-6′, H-7/H-6″, H-6"/H-5″, H-6"/H-1; **18** (Fig. S50): H-7/H-2″, H-7/H-6″, H-2"/OMe-3″, H-6"/H-5″, H-5"/OMe-4″, H-7/H-6′, H-6′/H-5′, H-5′/OMe-4′, H-5/H-2′, H-6"/H-1; **19** (Fig. S55): H-7/H-2″, H-2"/H-3″, H-3"/OMe-4″, H-7/H-2′, H-2′/OMe-3′, H-7/H-6′, H-6′/H-5′, H-5′/OMe-4′, H-5/H-2′, H-5/H- 6′ and H-6"/H-1.

The ^{13}C NMR data also showed the characteristics of 6,8-diaryl substituted tetrahydroindolizidine, including the signals of two aryl groups at C-6 and C-8 and indolizine at C-1, C-2, C-3, C-5 and C-7 in **16**–**19**. The IUPAC names of **16**–**19** were 6-(4-methoxyphenyl)-8-(4-hydroxyphenyl)-1,2,3-trihydro indolizidinium TFA salt (**16**), 6,8-*bis*(4,4-hydroxyphenyl)-1,2,3-trihydroindolizidinium acetate (**17**), 6-(4-methoxy-phenyl)-8-(4,5-dimethoxyphenyl)-1,2,3-trihydroindolizidinium TFA salt (**18**) and 6-(4,5-di methoxyphenyl)-8-(4-methoxyphenyl)-1,2,3-trihydro-indolizidinium TFA salt (**19**), respectively.

3.2.2. Structural elucidation of phenanthroindolizidines (6 and 10)

The molecular formula of **6** was determined as $C_{23}H_{24}NO_4$ by HR-ESIMS. The ^1H (Fig. S17) and ^{13}C (Fig. S18) NMR spectra of **6** showed the characteristic signals for a 2,3,6-trimethoxyphenanthroindolizidine, similar to a reported tetrahydroantofinium TFA salt (**14**) [26], except for an upfield peak at δ_H 5.76, and an aromatic signal at δ_H 8.03 in the tetrahydroantofinium. This suggests that the 13a,14-double (olefinic) bond was replaced by a hydroxy group on C-14. The

proposed structure was supported by the correlations observed in the 2D COSY (Fig. S19, H-11/H-12, H-12/H_2-13, H_2-13/H-13a, H-13a/H-14), NOESY (Fig. S20, H-1/OMe-2, H-1/H-14, H-4/OMe-3, H-5/OMe-6, H-7/OMe-6, H-7/H-8, H-8/H-9) and HMBC spectra. On the other hand, H-13a and H-14 (m, $J = 4.0$ Hz) were *cis* according to their coupling constants, and the stereochemistry of C-13a was an *S*-form according to its positive value of specific rotation [25]. In addition, the negative Cotton effect at 279 nm in the CD spectrum indicated the *S* form at both C-13a and C-14 (Fig. S22) [27]. Therefore, compound **6** is a new compound, identified as (13a*S*,14*S*)-14-hydroxy-2,3,6-trimethoxy-9-hydroantofinium TFA salt.

The molecular formula of **10** was determined as $C_{23}H_{22}NO_3$ by HR-ESIMS. The ^{1}H NMR spectrum of **10** (Table 3; Fig. S34) revealed an ABX system [δ_H 7.40 (dd, $J = 9.0$, 2.5 Hz, H-2), δ_H 7.63 (d, $J = 9.0$ Hz, H-1), δ_H 9.30 (d, $J = 2.5$ Hz, H-4)] and two *ortho*-coupled aromatic signals [δ_H 8.73, (d, $J = 9.1$ Hz, H-7), δ_H 8.66, (d, $J = 9.1$ Hz, H-8)]. In the aliphatic region, δ_H 2.61 (quin, $J = 7.7$ Hz, H-12), δ_H 3.63 (t, $J = 7.9$ Hz, H-13) and δ_H 4.97 (t, $J = 7.6$ Hz, H-11) belonged to the signals of a nitrogen-containing heterocyclic ring. The downfield signal at δ_H 4.97 t was assigned to H-11 because it was adjacent to *N*-10, and the upfield signal at 3.63 t was therefore assigned to H-13. Compounds **10** and **11** were positional isomers with different methoxy positions. The *O*-methyl groups on the B ring of **10** were on the C-5 and C-6 positions by the downfield H-4 at δ_H 9.30 (d, $J = 2.5$ Hz), which was affected by paramagnetic anisotropic effect and the nearby lone pair electrons of 5-*O* and was not seen in **11** (with its H-4 at δ_H 7.80). Accordingly, compound **10** was identified as 3,5,6-trimethoxy-11,12,13-trihyrodi-benzo [f,h] pyrrolo [1,2-b] isoquinoline and named tylophoridicine G.

3.3. Enhancing effect of the secondary metabolites on GLP-1 secretion

Effects of the 18 compounds on enhancing the secretion of glucagon-like receptor 1 (GLP-1) from STC-1 cells are shown in Fig. 3 (see Table S1 for data). Among these, 7 compounds (**3**, **6**, **13**, **14**, **15**, **16** and **26**) were mainly phenanthroindolizidine and indolizidine alkaloids, demonstrating GLP-1 enhancing effect at 50 mM (delta F value > 200), especially **14** and **6** [3.5- and 2.3-fold than the negative control (N.C.) (DMSO), respectively]. Other compounds, such as **15**, **3**, **16** and **13**, showed 1.3- to 2.3- fold greater enhancing effect than the N.C.

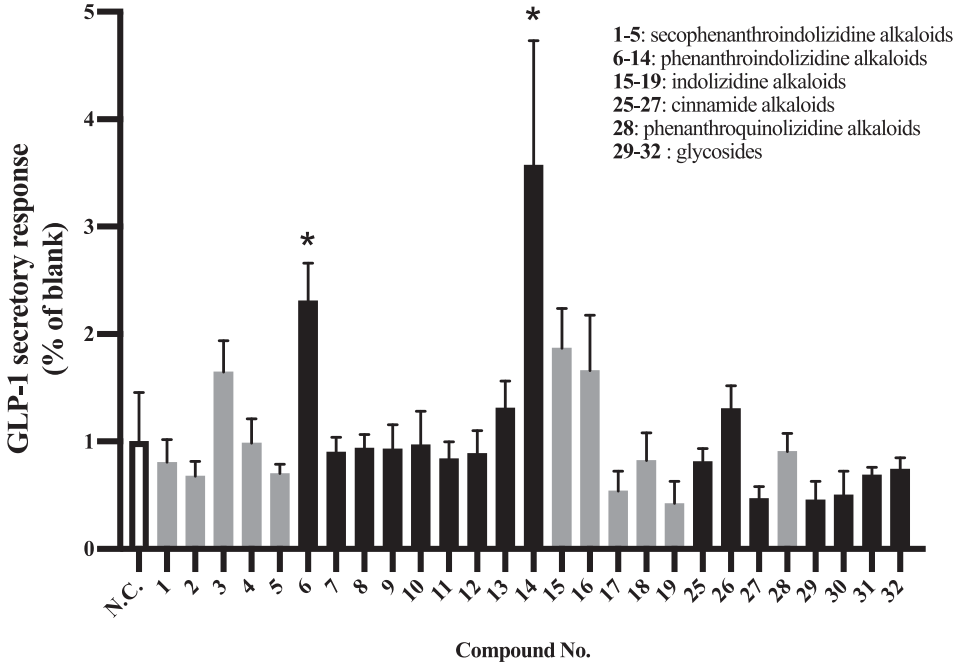

Fig. 3. Enhancing effect of the 27 isolated compounds on GLP-1 secretion from STC-1 cells (N.C.: negative control, DMSO) (: $p < 0.05$).*

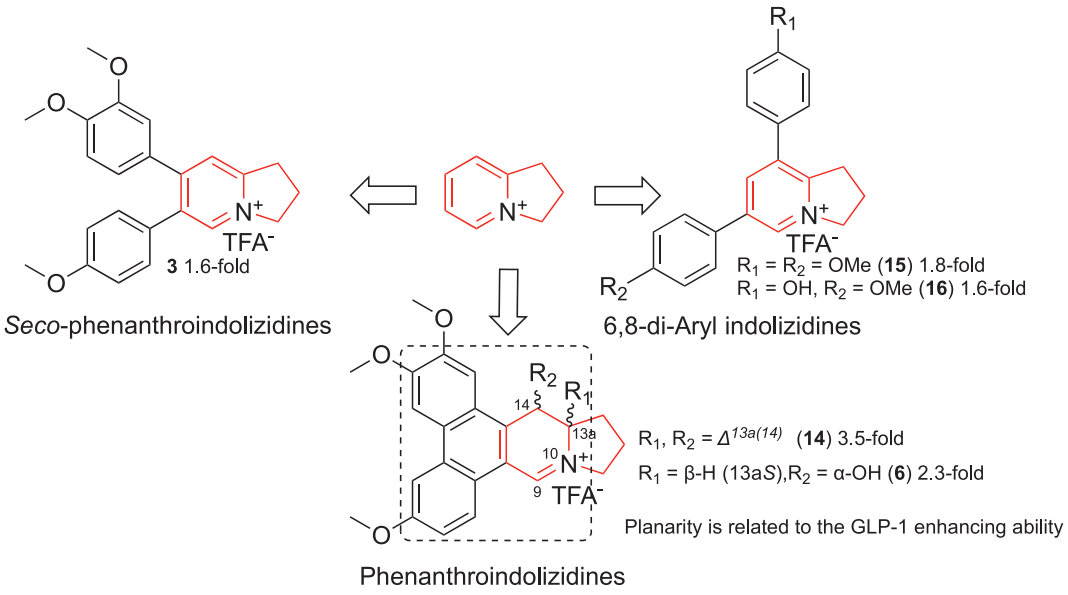

Fig. 4. Structure–activity relationship analysis of septicine-type, phenanthroindolizidine and indolizidine alkaloids.

4. Discussion

Among the phenanthroindolizidine-type alkaloids (**6**–**14**), **14** and **6** showed the strongest enhancing activity for GLP-1 secretion (Fig. 3). The factors that might affect the planarity of these compounds, such as the π-bonds between the *N*, C-13a, C-14, C-14a and C-8b positions, could contribute to enhancing the secretion of GLP-1. Of the *seco*-phenanthroindolizidine alkaloids **1**–**5**, compound **3** was the most potent. In indolizidine alkaloids (**15**–**19**), **15** and **16** were more potent, which may be related to the *para*-substituted methoxy and hydroxy groups. Other compounds, including cinnamamides (**25**–**27**) and glycosides (**29**–**32**), showed only weak activity to enhance the secretion of GLP-1 in this study (Fig. 3).

Structure–activity relationship of the three indolizidine alkaloids (*seco*-phenanthroindolizidine, phenanthroindolizidine and 6,8-di-aryl indolizidine) was analyzed. Chemical skeletons of the top five active alkaloids (**3**, **6**, **14**, **15** and **16**) had increased compared to the negative control (DMSO) in Fig. 4. All of the five active compounds are quaternary amine TFA salts. The two compounds with a 2,3,6-tri-*O*-methyl phenanthroindolizidine skeleton and with $\Delta^{13a(14)}$ (**14**) or 13a*S*,14α-OH (**6**) functional groups showed the highest potency (3.5- and 2.3-fold, respectively); the other three showed a similar potency of around 1.7-fold, for both 2,3,6-tri-*O*-methyl *seco*-phenanthroindolizidine (**3**) and 6,8-di-aryl indolizidine (**15** and **16**) alkaloids. This shows that the structural planarity of these compounds was related to their ability to enhance GLP-1. Of the indolizidine alkaloids, the *para*-substituted methoxy groups could increase the secretion of GLP-1 (**15** and **16**) alkaloids. Replacement with hydroxy groups in the *para*-positions might result reduce GLP-1 enhancing ability (**17**). Comparing the results of **15**, **18** and **19** shows that the substitution of methoxy groups on the C-5′ or C-3″ position can reduce the secretion of GLP-1 (Fig. 4).

Many of these GLP-1-enhancing alkaloids also demonstrated other bioactivities. For example, **3** demonstrated anti-malaria activity, particularly to 3D7 *P. falciparum* strains (IC_{50} = 4.0 μM) [28]; **14** inhibits the growth of H9 cells infected by HIV (EC_{50} 1.88 μg/mL) [24]; **15** revealed inhibitory activity of *Bacillus subtilis* with a minimal concentration of 15 nM [23].

Declaration of competing interest

The authors declare no conflicts of interest.

Acknowledgments

This work was supported by the grants MOST 106-2320-B-002-012-MY3 (to CCC) and MOST106-2320-B002-009-MY3 (SSL) from the National Science and Technology Council, Taiwan, Republic of China. The authors also thank Dr. Shing-Jong Huang of the Instrumentation Center, National Taiwan University, for assistance in the 800 MHz NMR experiments.

Appendix. Supporting information

Supplementary materials

*Table S1. GLP-1 enhancing ability of compounds **1**–**32**. (Secretory response, % of blank)*

Septicine-type (*seco*-phenanthroindolizidine) alkaloids	**1**	**2**	**3**	**4**	**5**	**DMSO**
	0.81 ± 0.34	0.67 ± 0.21	1.65 ± 0.46	0.99 ± 0.98	0.71 ± 0.70	1.00
Phenanthroindolizidine alkaloids	**6**	**7**	**8**	**9**		**10**
	2.31 ± 0.56	0.90 ± 0.44	0.93 ± 0.41	0.93 ± 0.73		1.01 ± 0.97
	11	**12**	**13**	**14**		
	0.83 ± 0.51	0.89 ± 0.70	1.31 ± 0.4	3.57 ± 1.85		
Indolizidine alkaloids	**15**	**16**	**17**	**18**		**19**
	1.87 ± 0.59	1.66 ± 0.82	0.54 ± 0.29	0.82 ± 0.41		0.42 ± 0.33
Cinnamaide alkaloids	**25**	**26**	**27**	**Phenanthroqunolizidine alkaloids**		**28**
	0.82 ± 0.19	1.30 ± 0.34	0.47 ± 0.18			0.91 ± 0.55
Glycosides	**29**	**30**	**31**	**32**		
	0.46 ± 0.27	0.50 ± 0.35	0.69 ± 0.11	0.74 ± 0.17		

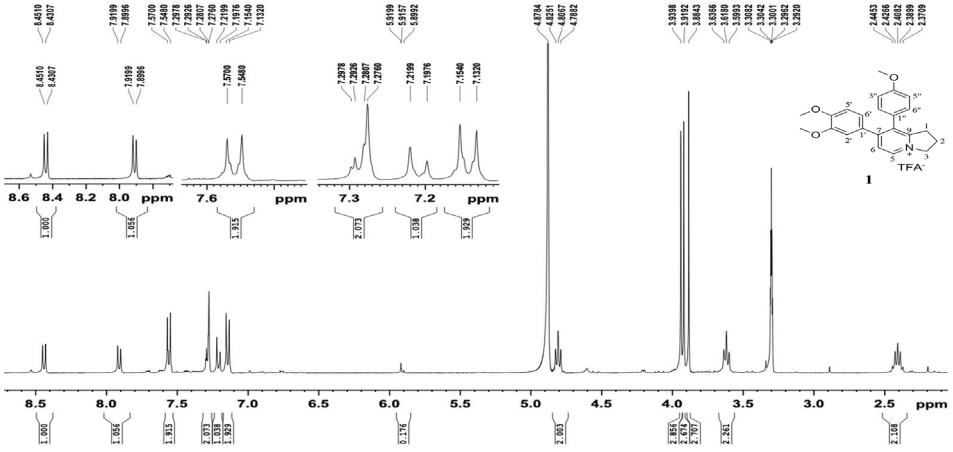

*Fig. S1. ^{1}H NMR spectrum of compound **1** (CD_3OD, 400 MHz).*

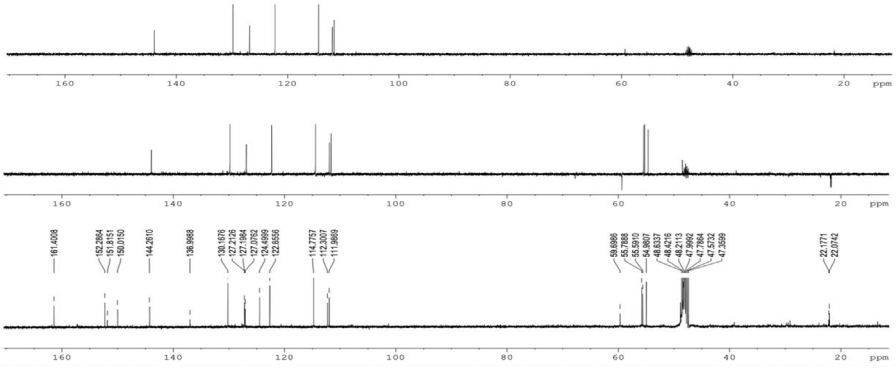

*Fig. S2. ^{13}C NMR spectrum of compound **1** (BBD, bot.; DEPT-135, mid.; DEPT-90, top) (CD_3OD, 100 MHz).*

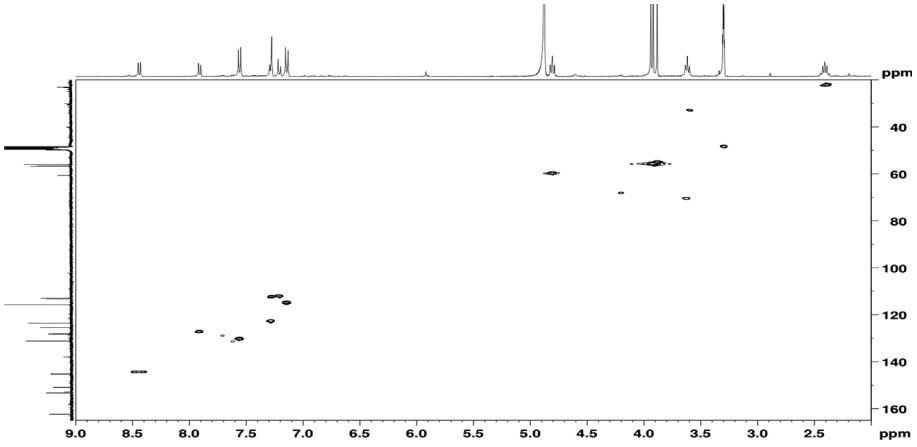

Fig. S3. HSQC spectrum of compound **1** *(CD_3OD, 600 MHz).*

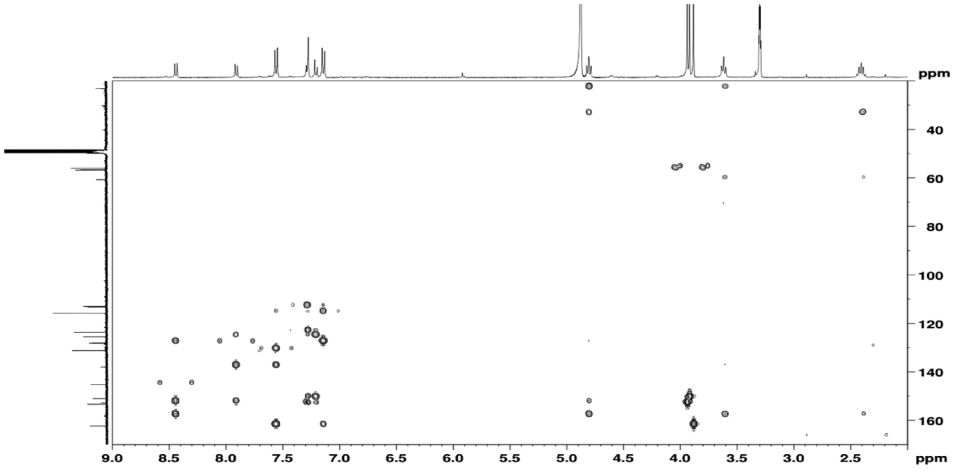

Fig. S4. HMBC spectrum of compound **1** *(CD_3OD, 600 MHz).*

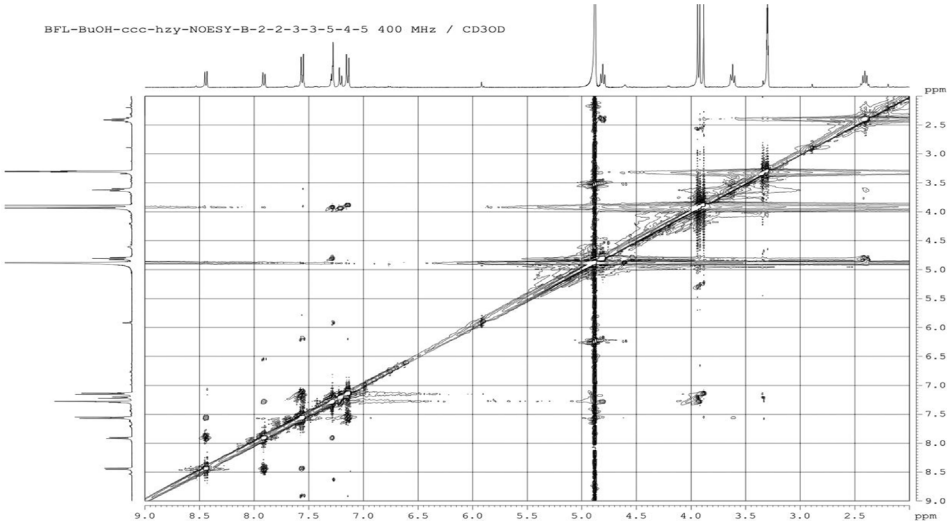

Fig. S5. NOESY spectrum of compound **1** *(CD_3OD, 600 MHz).*

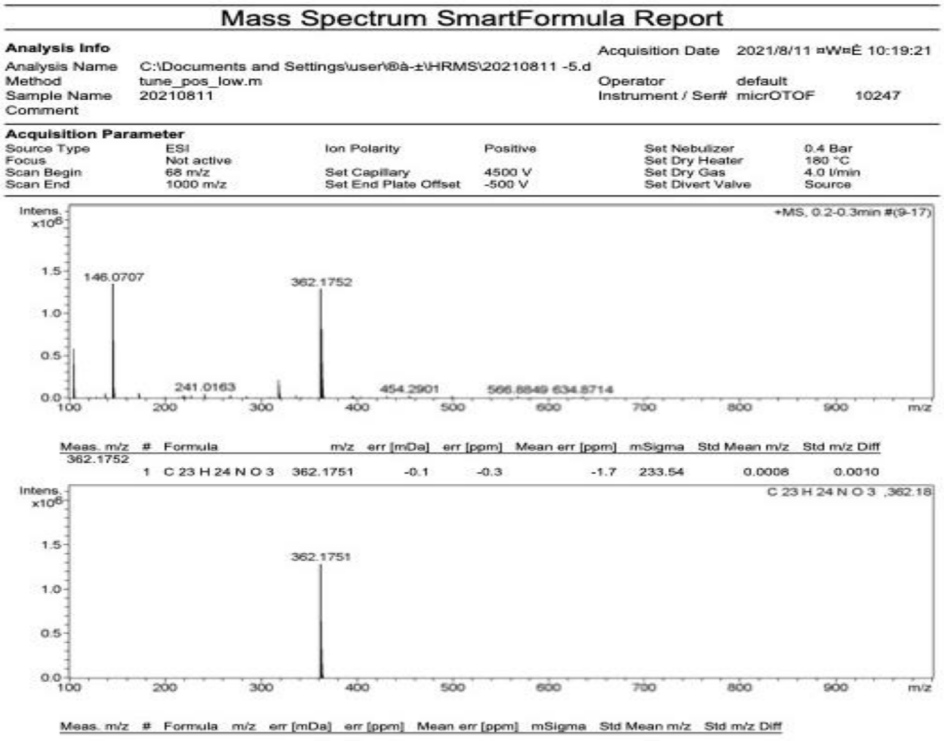

*Fig. S6. HR-ESI-MS spectrum of compound **1**.*

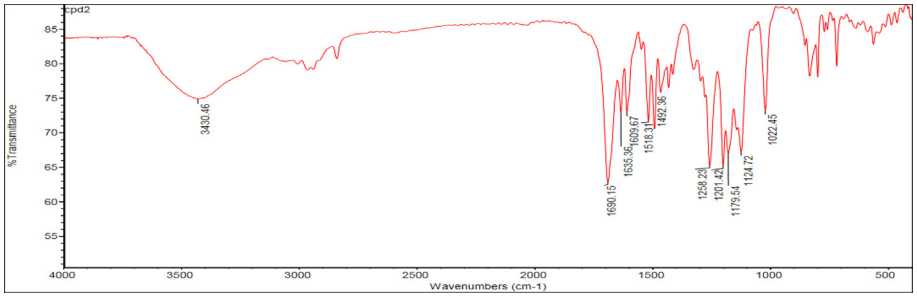

*Fig. S7. IR spectrum of compound **1**.*

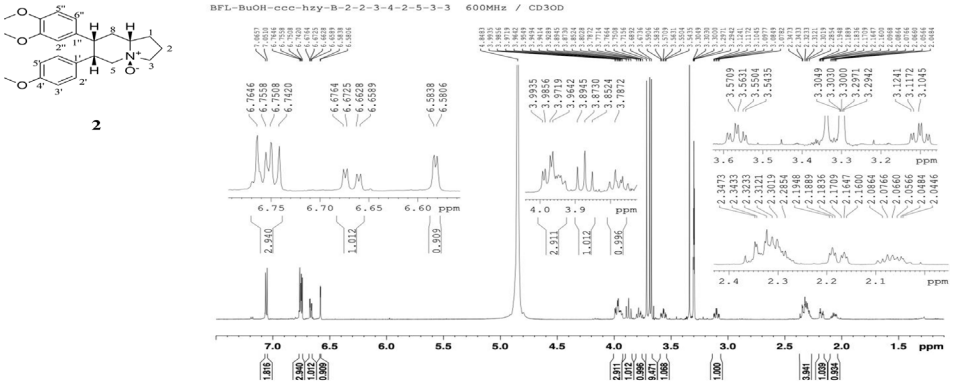

*Fig. S8. ^{1}H NMR spectrum of compound **2** (CD_3OD, 600 MHz).*

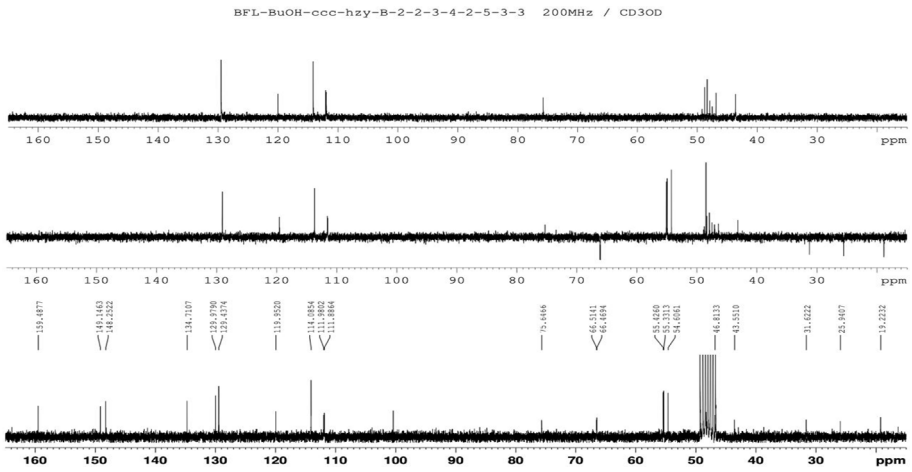

*Fig. S9. ^{13}C NMR spectra of compound **2** (BBD, bot.; DEPT-135, mid.; DEPT-90, top) (CD_3OD, 50 MHz).*

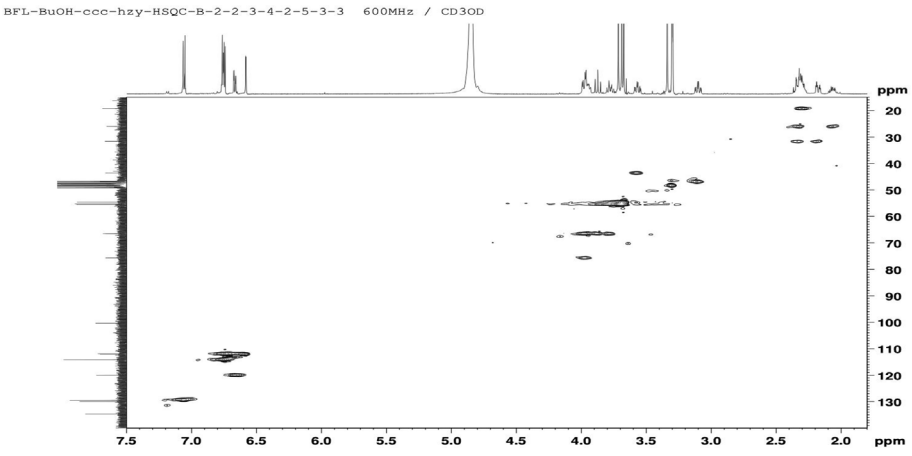

*Fig. S10. HSQC spectrum of compound **2** (CD_3OD, 600 MHz).*

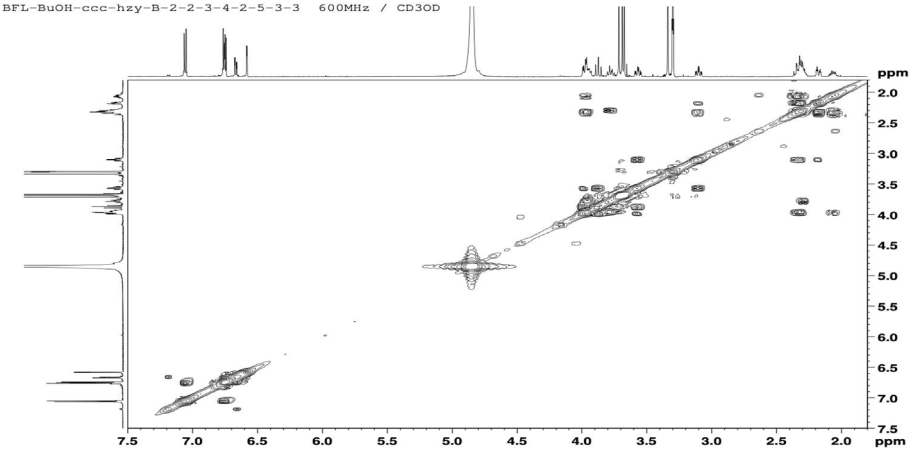

*Fig. S11. COSY spectrum of compound **2** (CD_3OD, 600 MHz).*

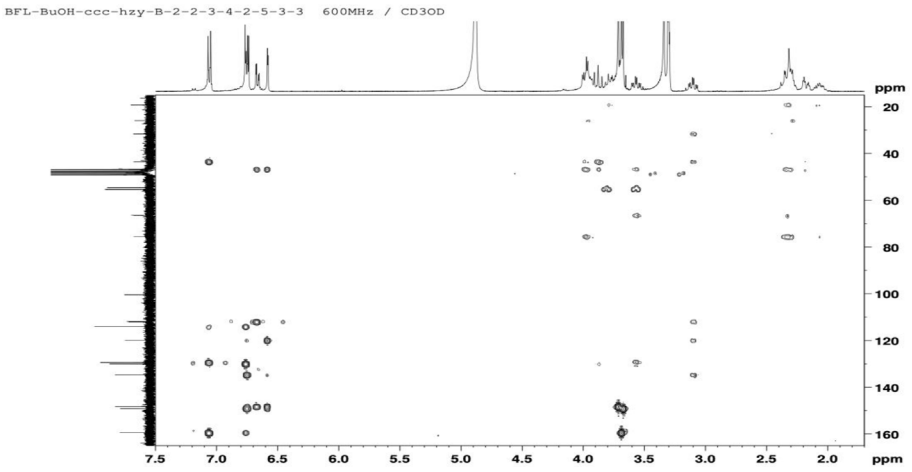

Fig. S12. HMBC spectrum of compound **2** *(CD_3OD, 600 MHz).*

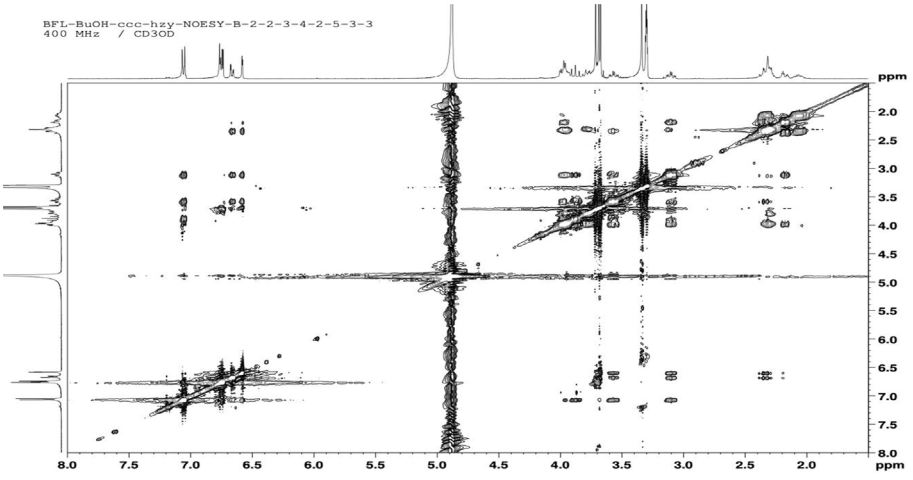

Fig. S13. NOSEY spectrum of compound **2** *(CD_3OD, 400 MHz).*

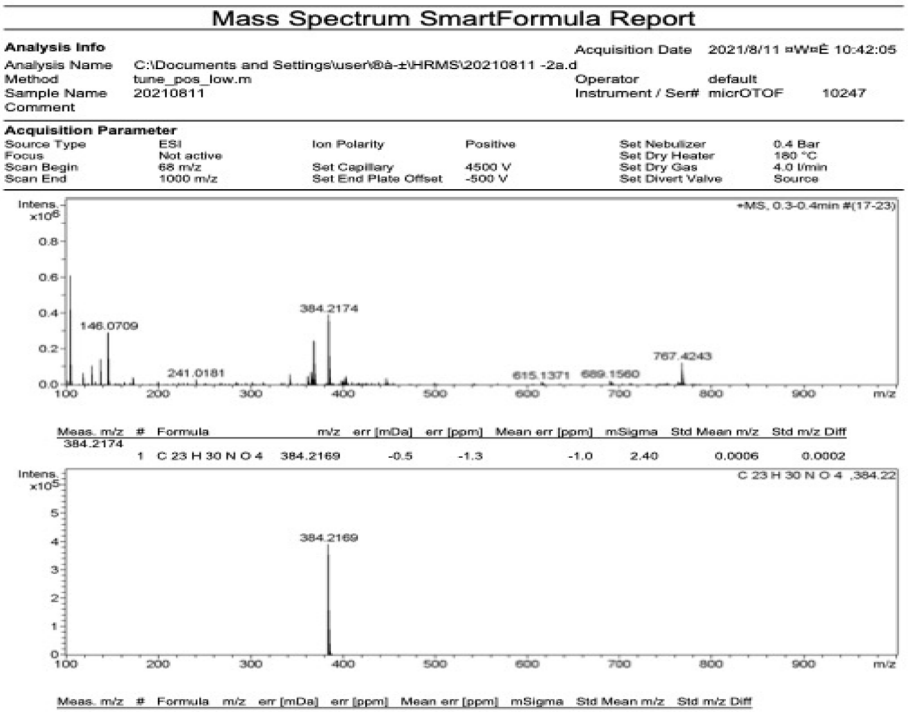

Fig. S14. HR-ESI-MS spectrum of compound 2.

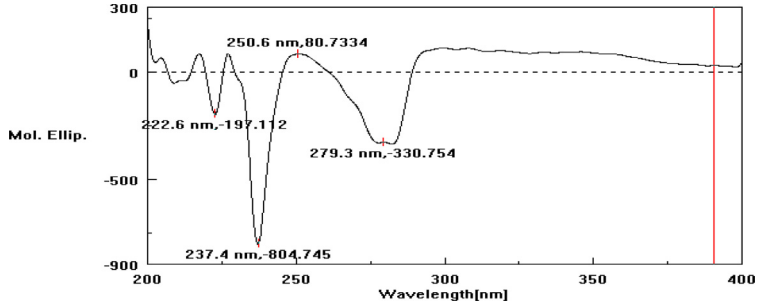

Fig. S15. CD spectrum of compound 2.

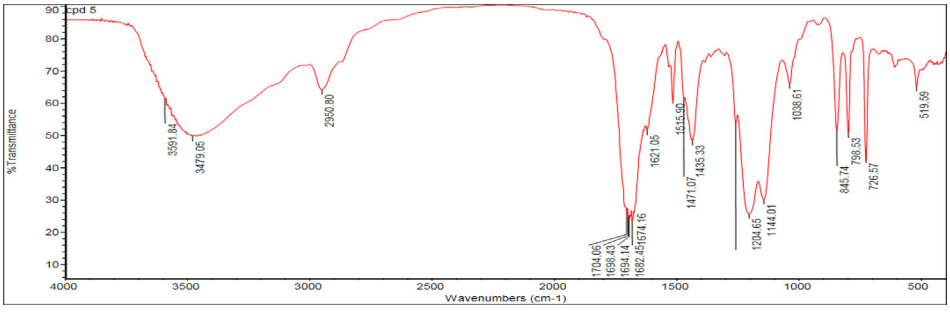

Fig. S16. IR spectrum of compound 2.

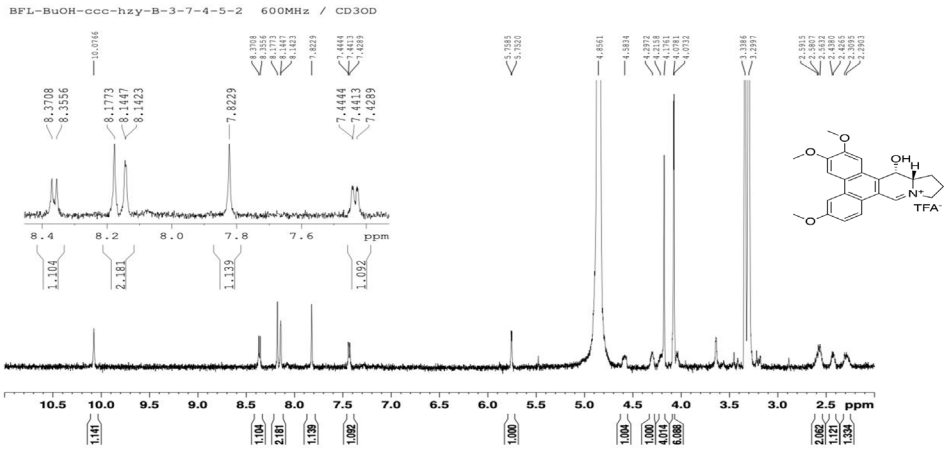

*Fig. S17. ^{1}H NMR spectrum of compound **6** (CD_3OD, 600 MHz).*

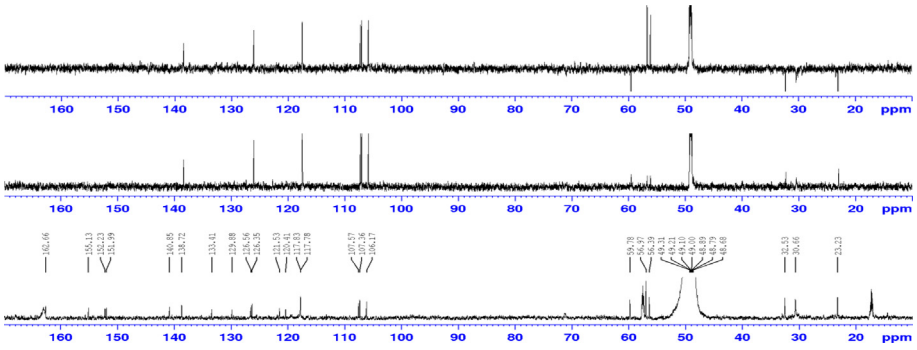

*Fig. S18. ^{13}C NMR spectra of compound **6** (BBD, bot.; DEPT-90, mid.; DEPT-135, top) (CD_3OD, 200 MHz).*

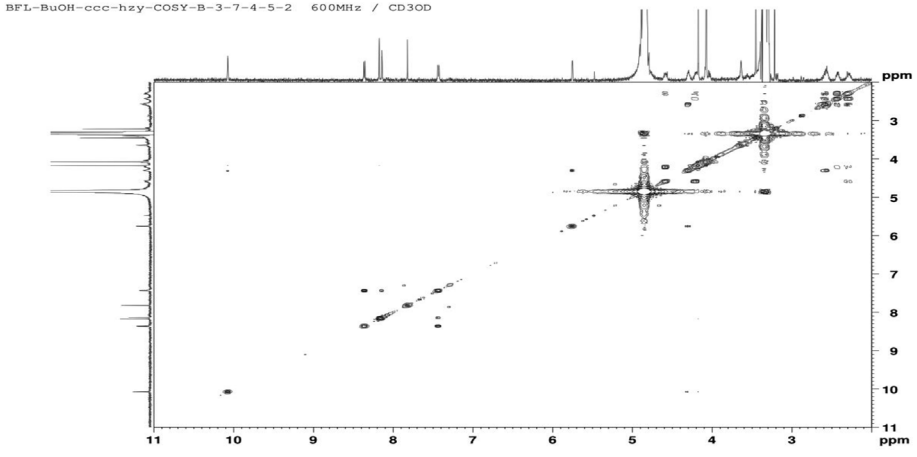

*Fig. S19. COSY spectrum of compound **6** (CD_3OD, 600 MHz).*

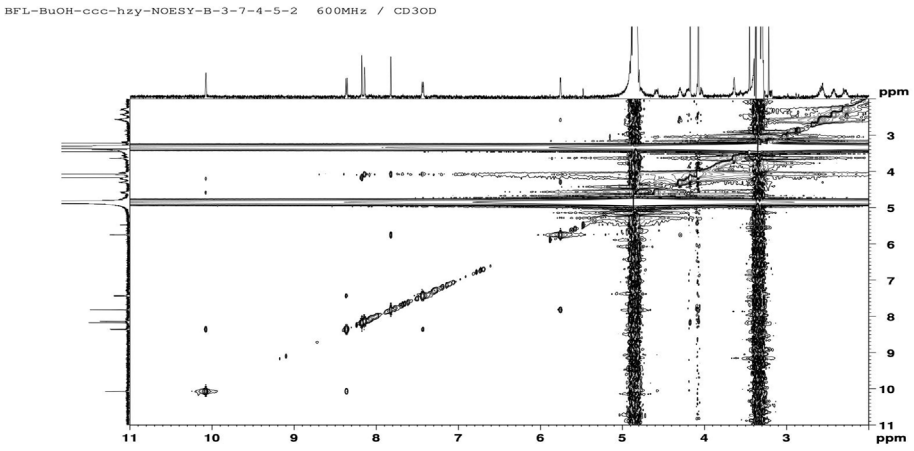

*Fig. S20. NOESY spectrum of compound **6** (CD_3OD, 600 MHz).*

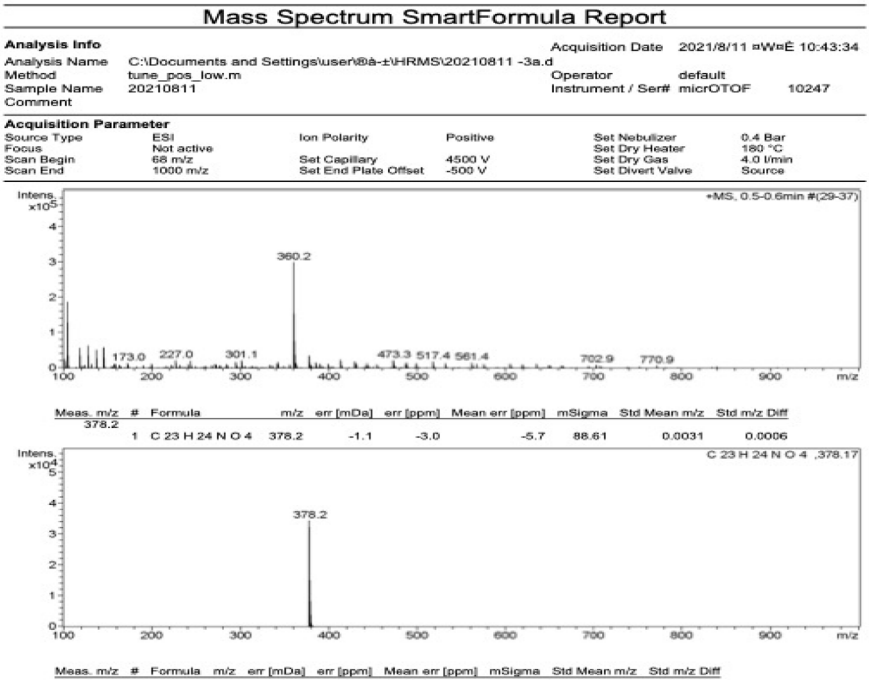

*Fig. S21. HR-ESI-MS spectrum of compound **6**.*

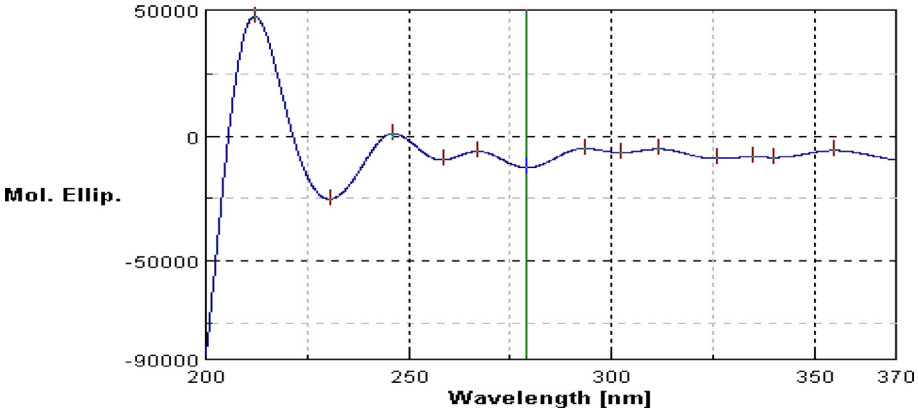

*Fig. S22. CD spectrum of compound **6**.*

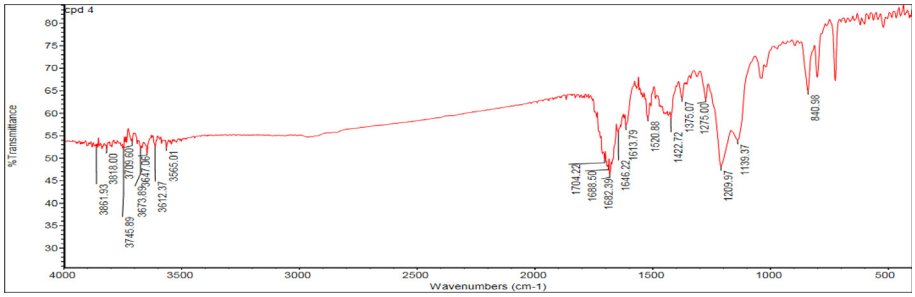

Fig. S23. IR spectrum of compound 6.

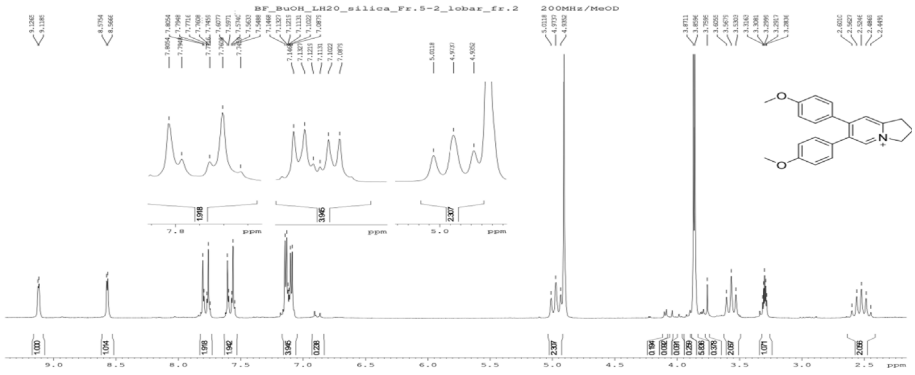

Fig. S24. ^{1}H NMR spectrum of compound 7 (CD_3OD, 200 MHz).

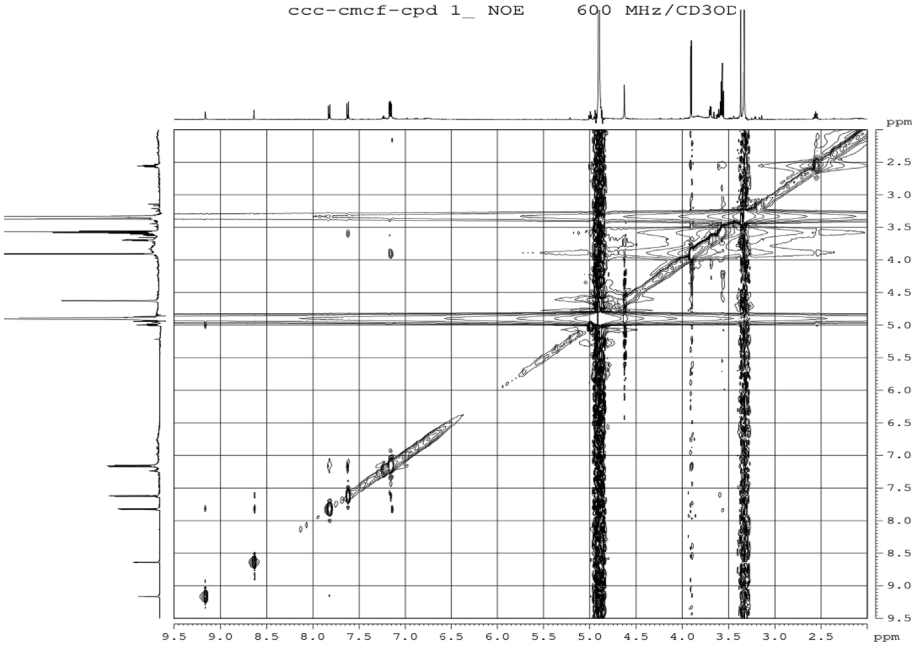

Fig. S25. NOESY spectrum of compound 7 (CD_3OD, 600 MHz).

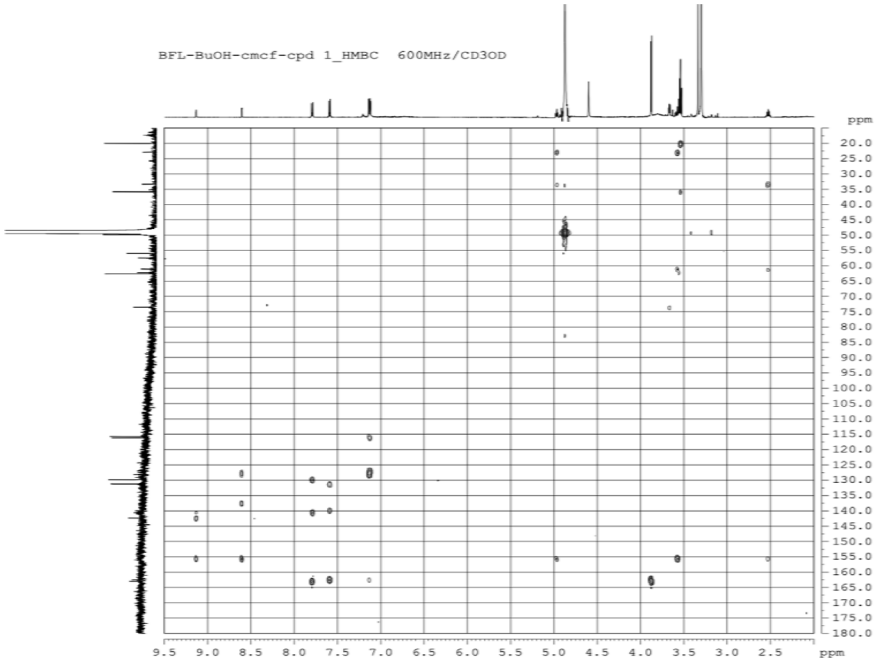

Fig. S26. HMBC spectrum of compound 7 (CD_3OD, 600 MHz).

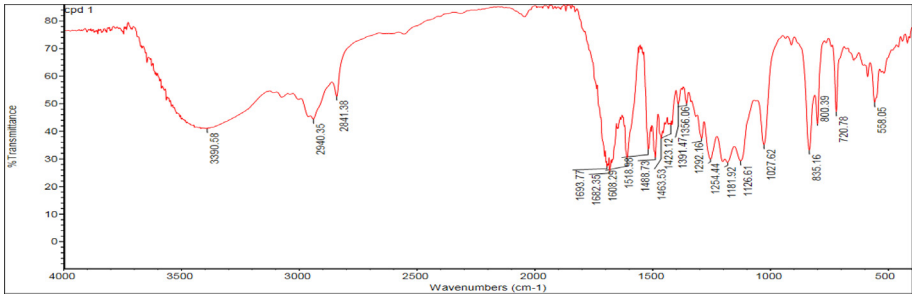

Fig. S27. IR spectrum of compound 7.

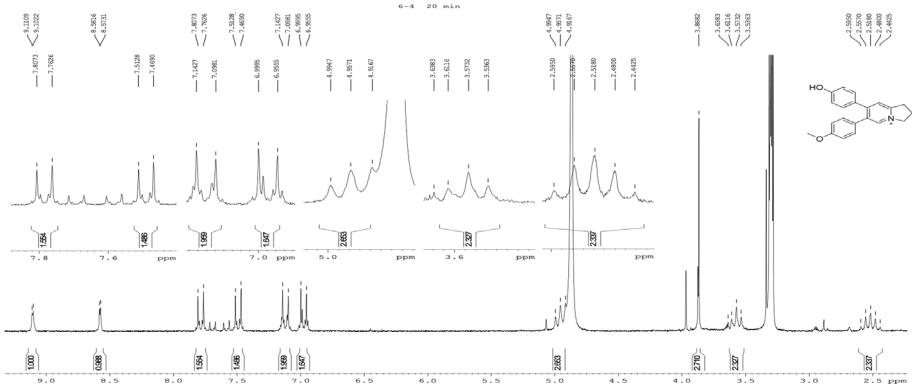

Fig. S28. ^1H NMR spectrum of compound 8 (CD_3OD, 200 MHz).

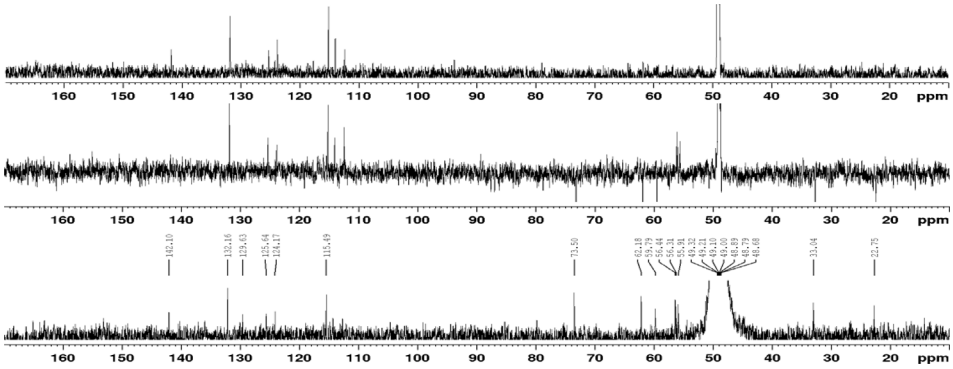

Fig. S29. ^{13}C spectrum of compound 8 (BBD, bot.; DEPT-135, mid.; DEPT-90, top) (CD3OD, 200 MHz) (CD_3OD, 200 MHz).

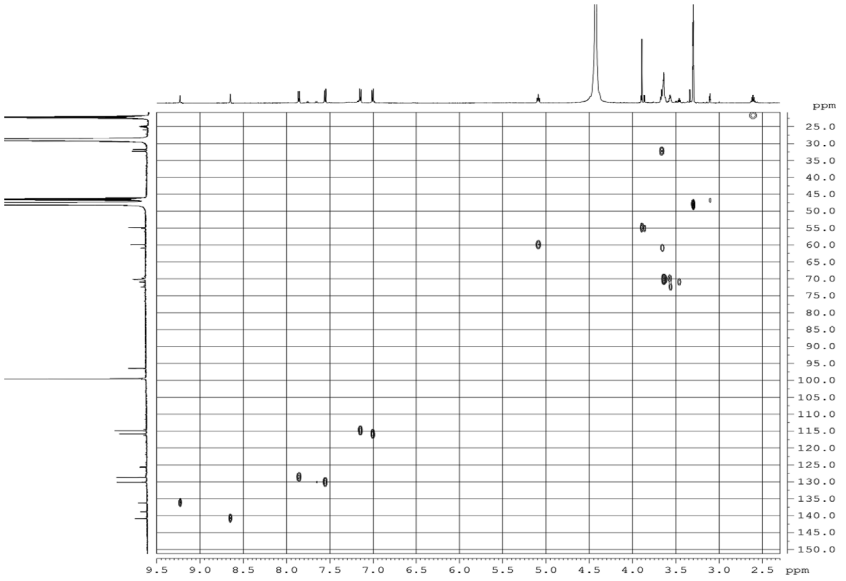

Fig. S30. HSQC spectrum of compound 8 (CD_3OD, 200 MHz).

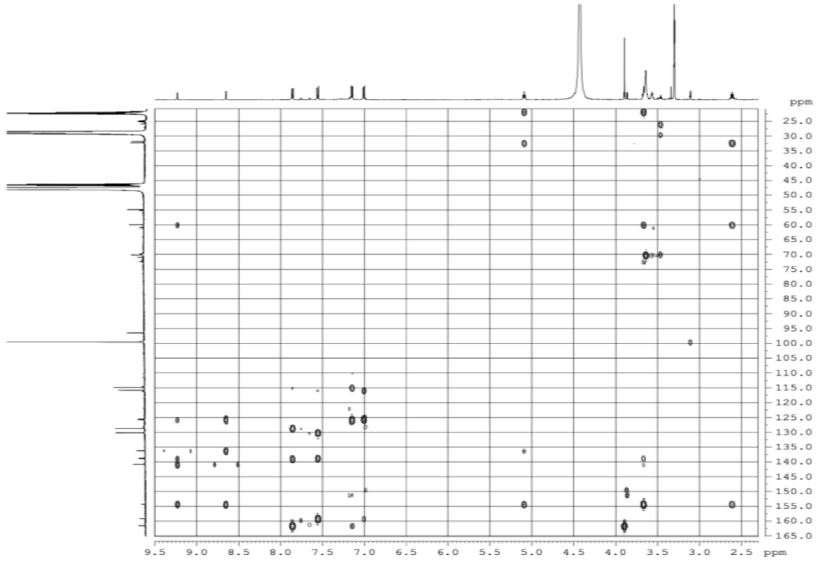

Fig. S31. HMBC spectrum of compound 8 (CD_3OD, 200 MHz).

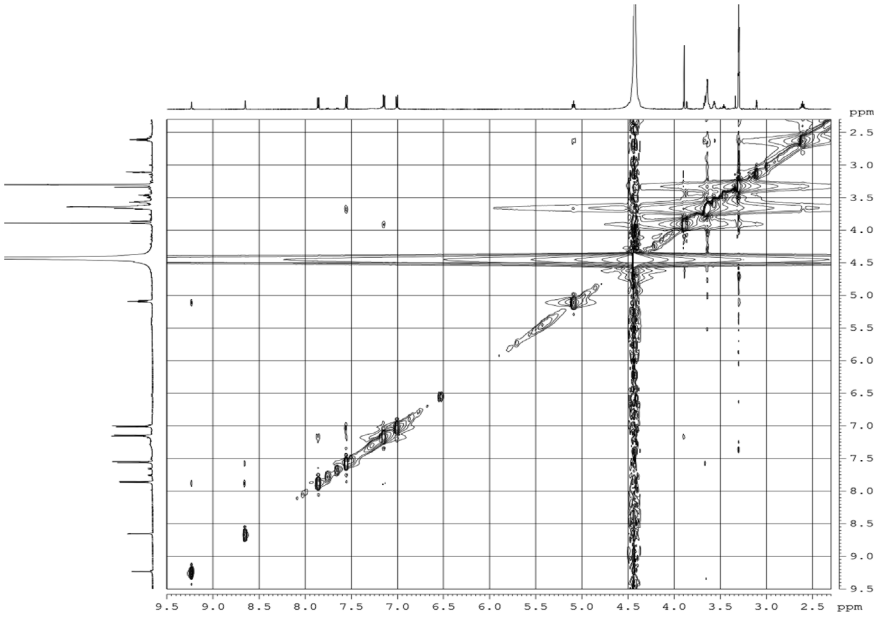

Fig. S32. NOESY spectrum of compound 8 (CD_3OD, 200 MHz).

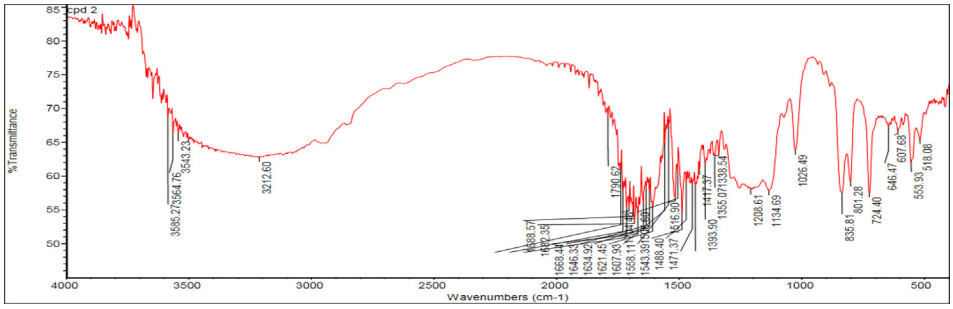

Fig. S33. IR spectrum of compound 8.

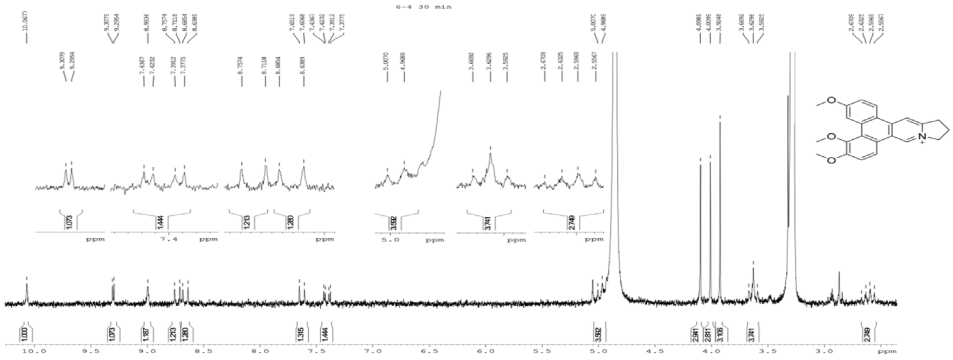

*Fig. S34. ^1H NMR spectrum of compound **10** (CD_3OD, 200 MHz).*

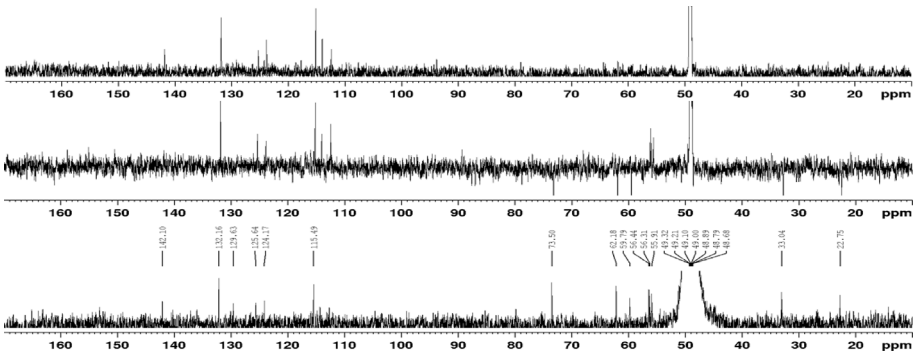

*Fig. S35. ^{13}C NMR spectrum of compound **10** (BBD, bot.; DEPT-135, mid.; DEPT-90, top) (CD_3OD, 100 MHz).*

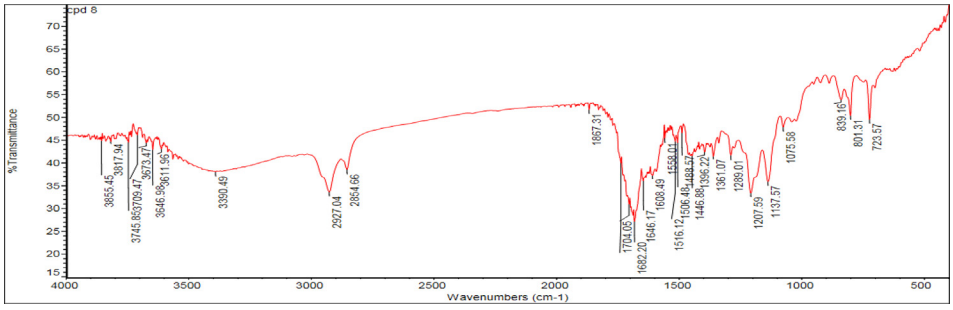

*Fig. S36. IR spectrum of compound **10**.*

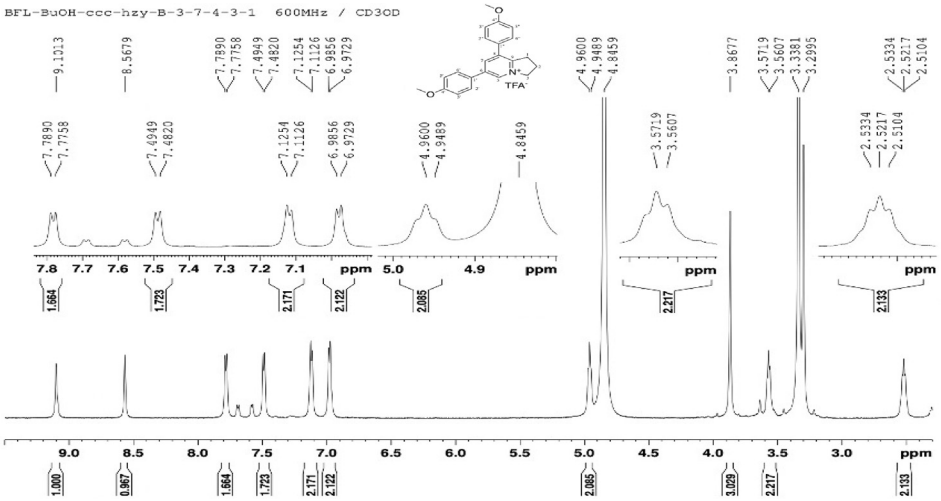

*Fig. S37. ^{1}H NMR spectrum of compound **16** (CD_3OD, 600 MHz).*

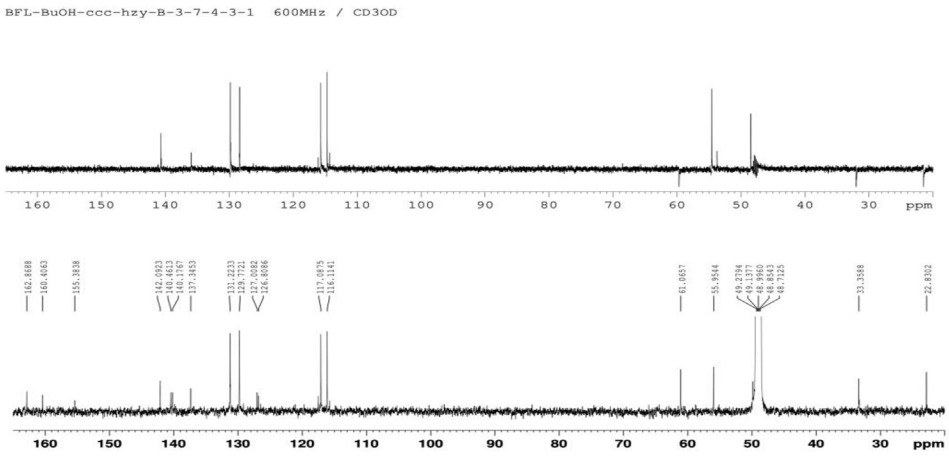

*Fig. S38. ^{13}C NMR spectrum of compound **16** (BBD, bot.; DEPT-135, top) (CD_3OD, 150 MHz).*

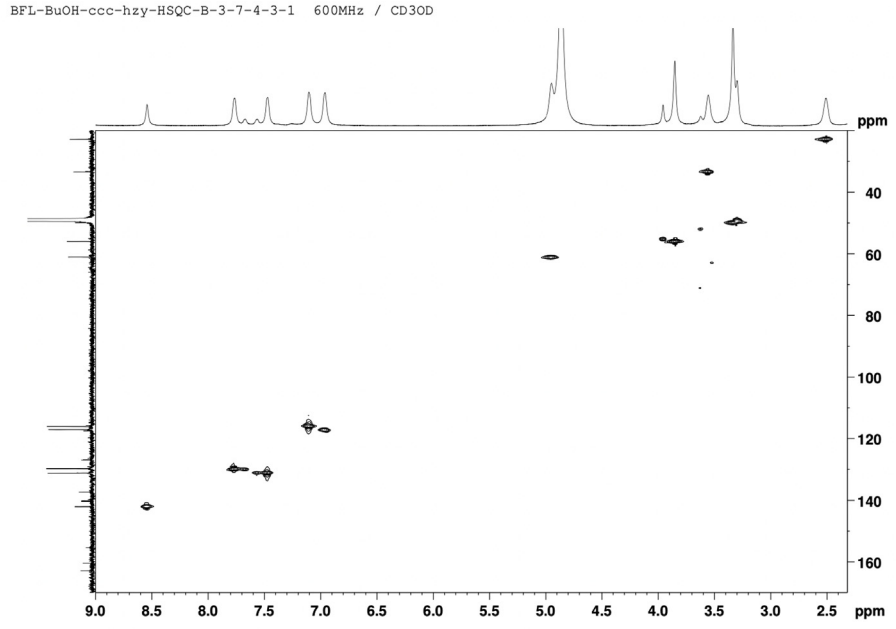

*Fig. S39. HSQC spectrum of compound **16** (CD_3OD, 600 MHz).*

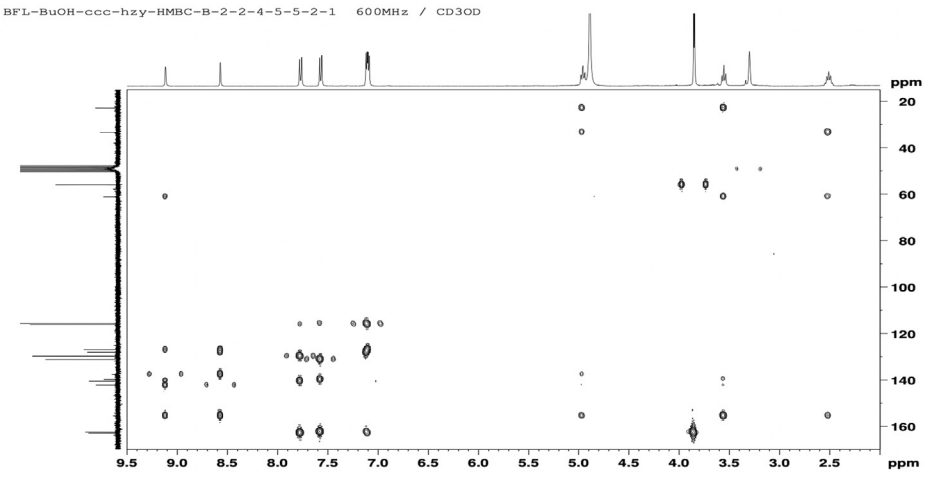

*Fig. S40. HMBC spectrum of compound **16** (CD_3OD, 600 MHz).*

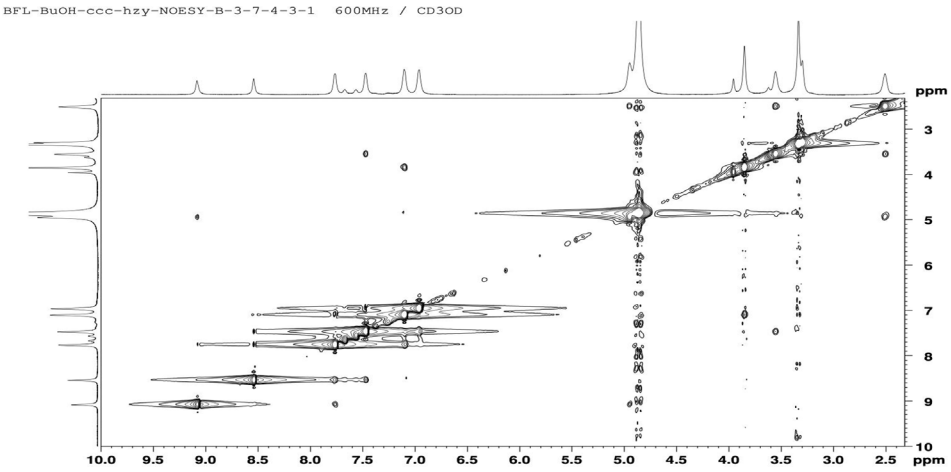

*Fig. S41. NOESY spectrum of compound **16** (CD_3OD, 600 MHz).*

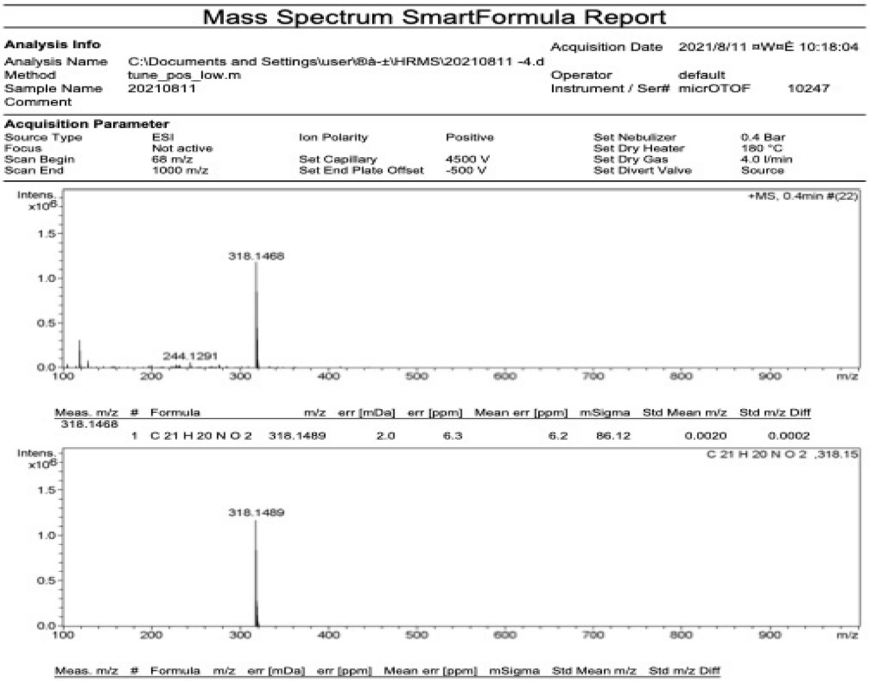

*Fig. S42. HR-ESI-MS spectrum of compound **16**.*

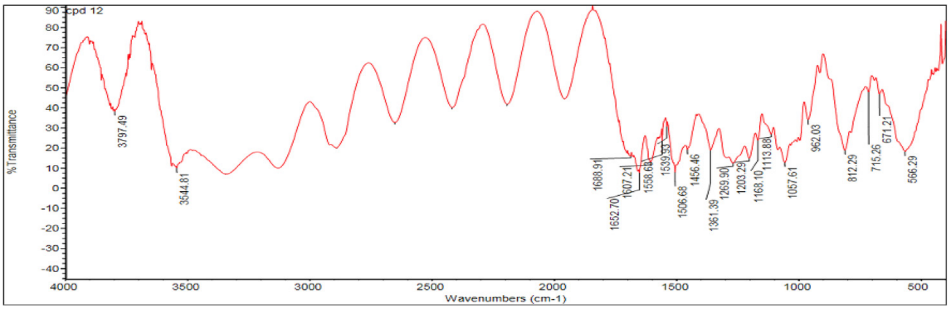

*Fig. S43. IR spectrum of compound **16**.*

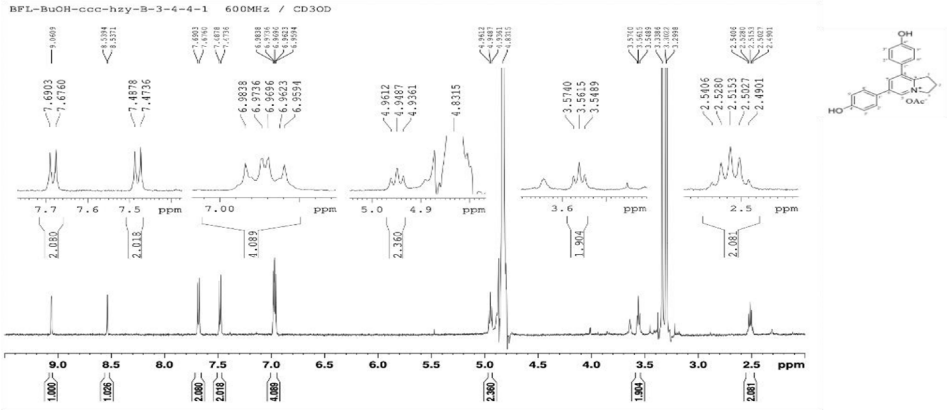

*Fig. S44. ^{1}H NMR spectrum of compound **17** (CD_3OD, 600 MHz).*

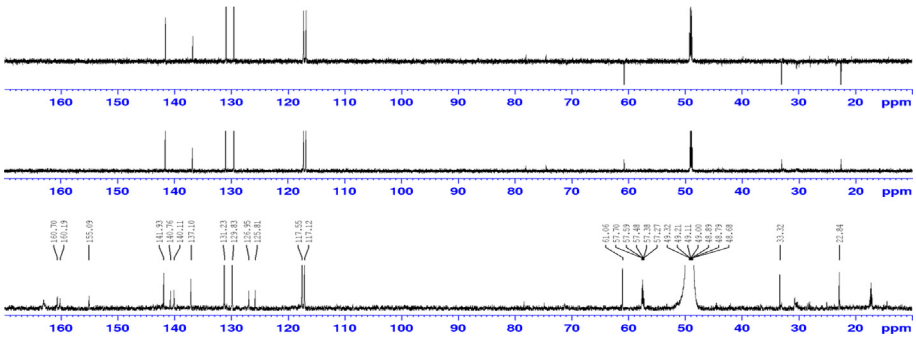

*Fig. S45. ^{13}C NMR spectrum of compound **17** (BBD, bot.; DEPT-90, mid.; DEPT-135, top) (CD_3OD, 200 MHz).*

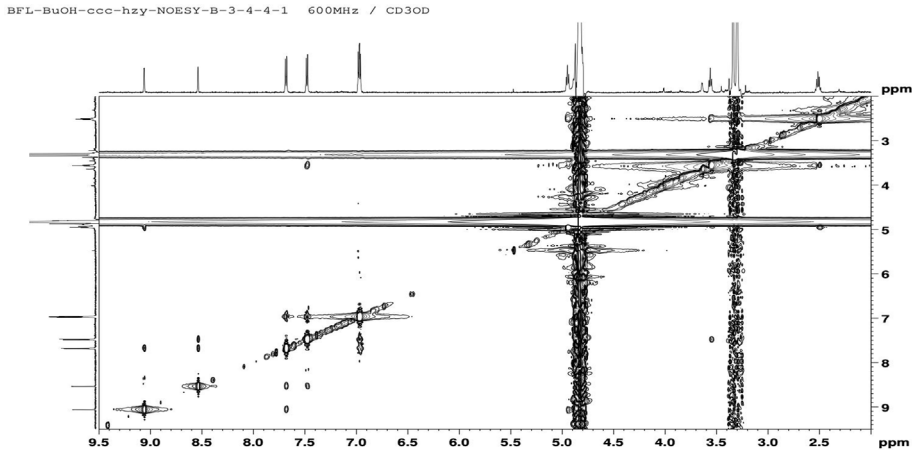

*Fig. S46. NOESY spectrum of compound **17** (CD_3OD, 600 MHz).*

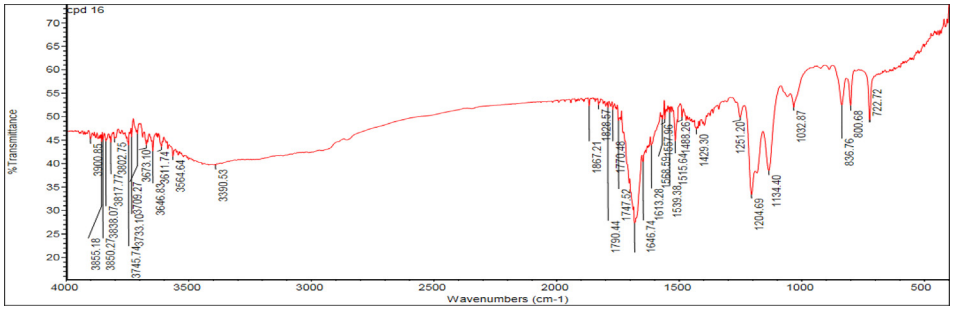

*Fig. S47. IR spectrum of compound **17**.*

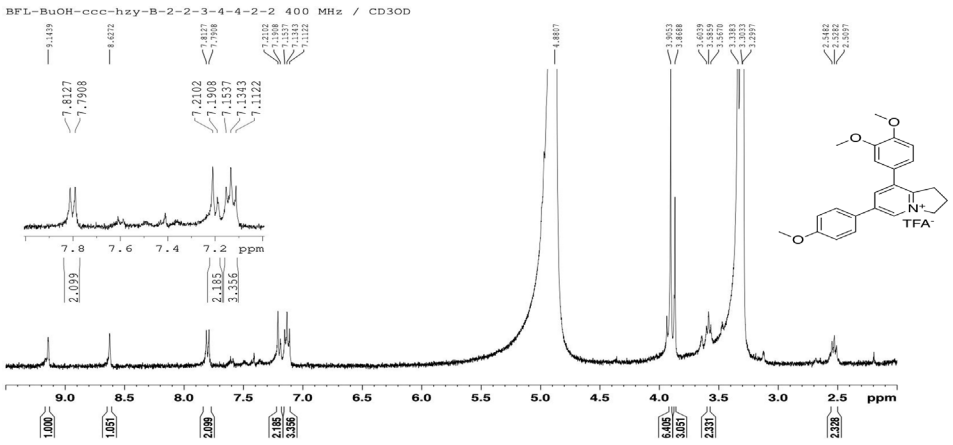

*Fig. S48. ^{1}H NMR spectrum of compound **18** (CD_3OD, 400 MHz).*

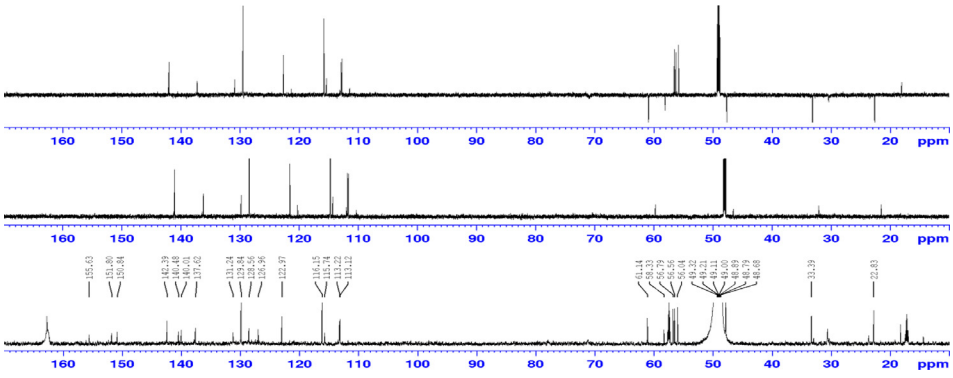

*Fig. S49. ^{13}C NMR spectrum of compound **18** (BBD, bot.; DEPT-90, mid.; DEPT-135, top) (CD_3OD, 200 MHz).*

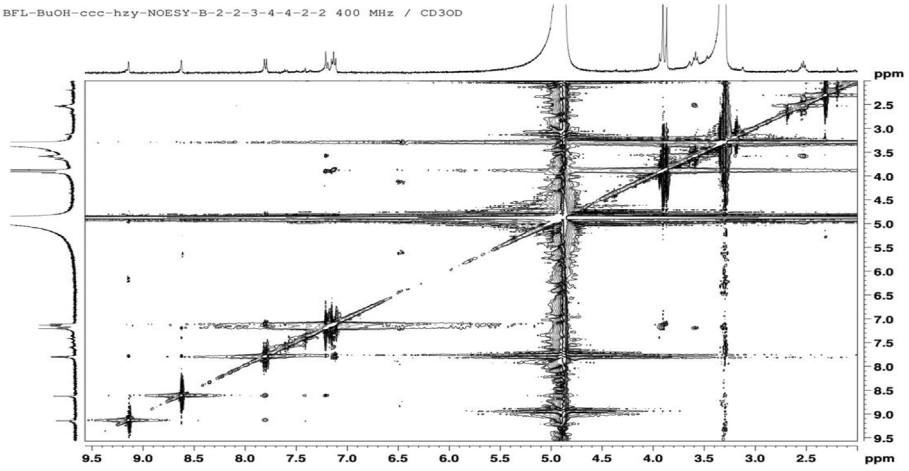

*Fig. S50. NOESY spectrum of compound **18** (CD_3OD, 400 MHz).*

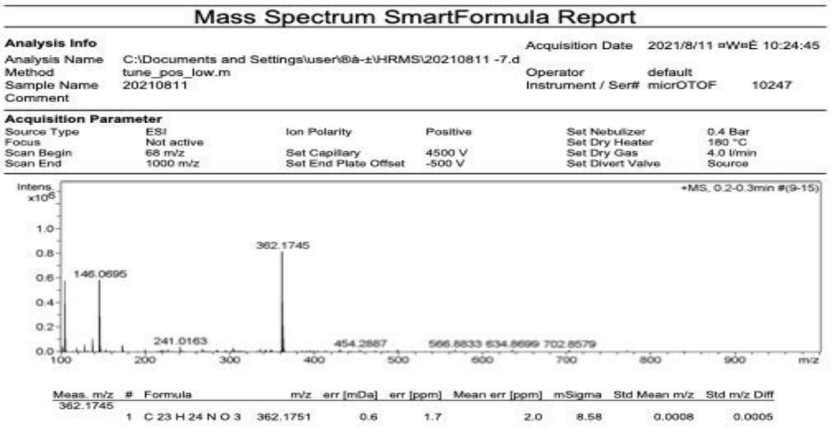

*Fig. S51. HR-ESI-MS spectrum of compound **18**.*

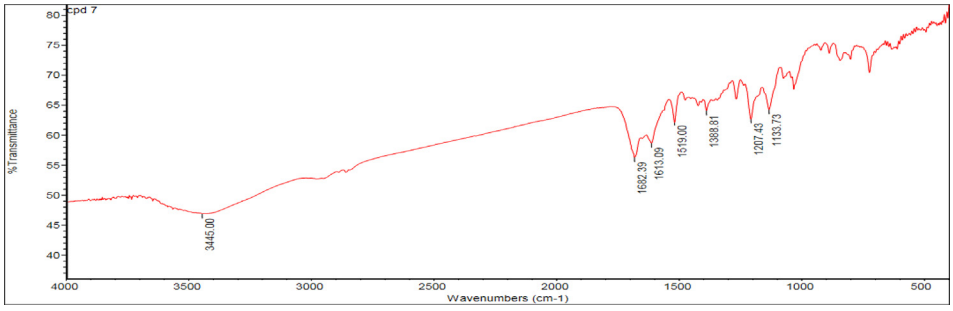

*Fig. S52. IR spectrum of compound **18**.*

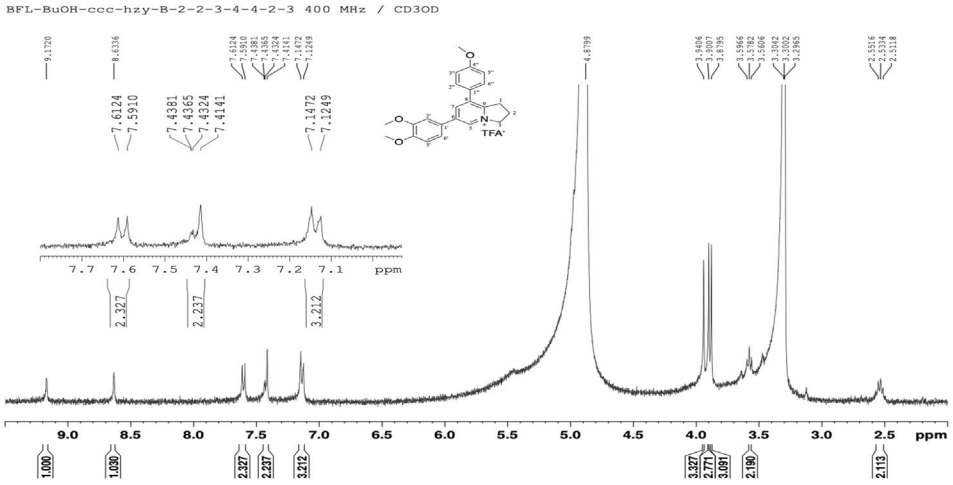

*Fig. S53. ^{1}H NMR spectrum of compound **19** (CD_3OD, 400 MHz).*

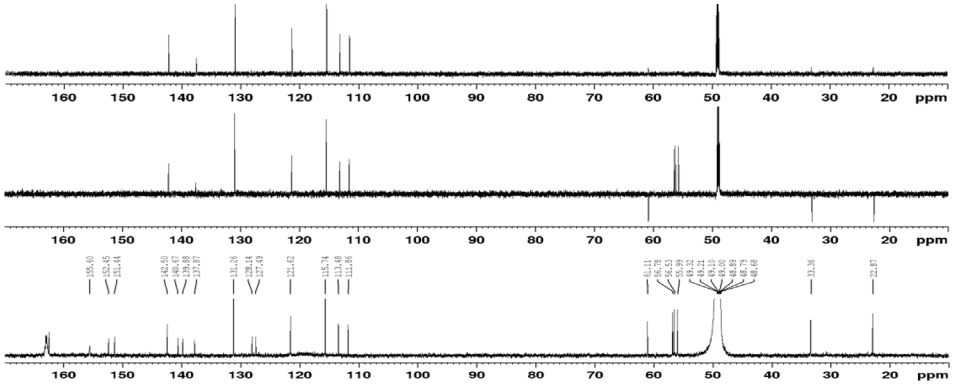

*Fig. S54. ^{13}C NMR spectrum of compound **19** (CD_3OD, 200 MHz) (BBD, bot.; DEPT-135, mid.; DEPT-90, top).*

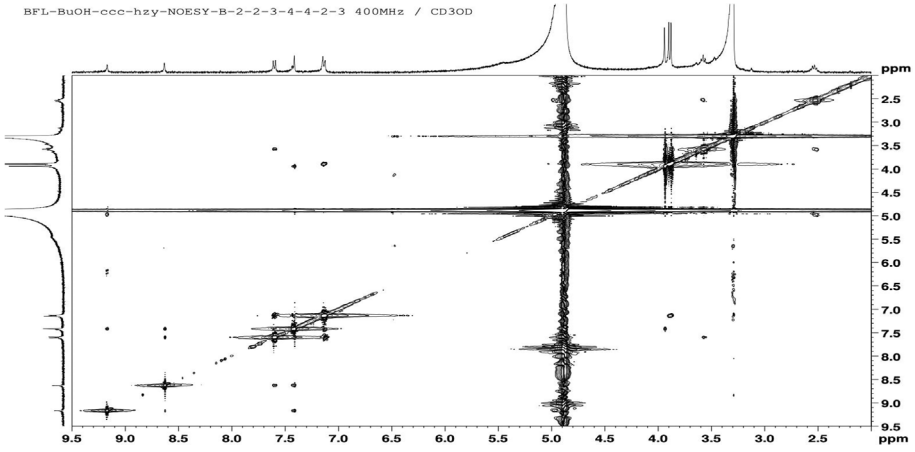

*Fig. S55. NOESY spectrum of compound **19** (CD_3OD, 400 MHz).*

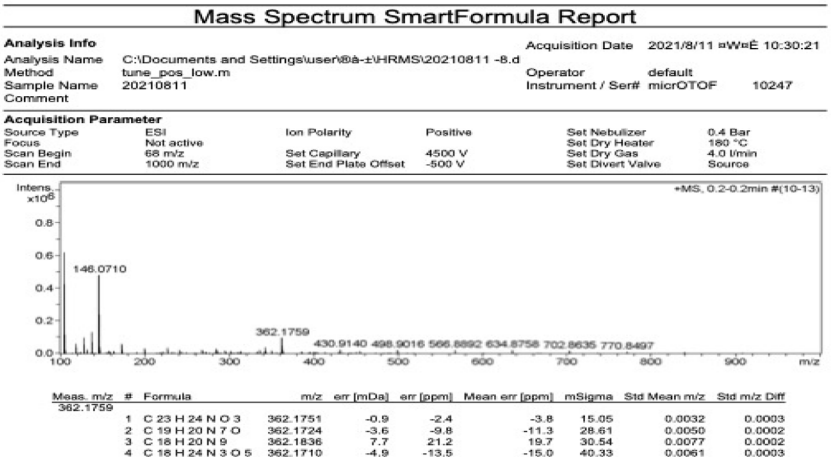

*Fig. S56. HR-ESI-MS spectrum of compound **19**.*

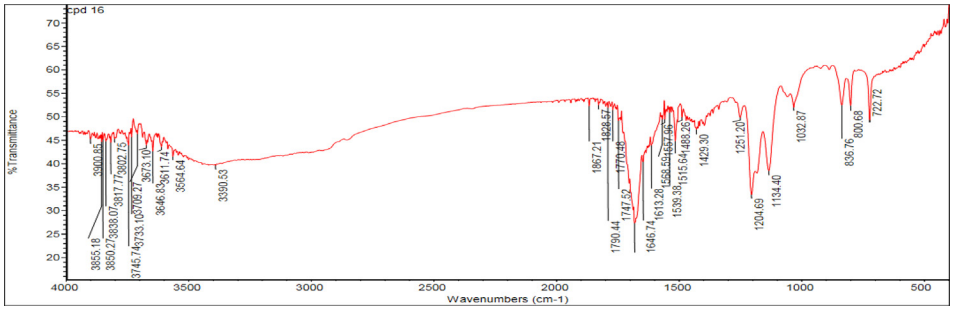

*Fig. S57. IR spectrum of compound **19**.*

Other Data

Isolation of known compounds

Isolation of known compounds from B. formasana leaf EtOH extract under light circumstance

Compounds **4**, **5**, **12** and **28** were isolated from Fr. 7-2. (116.1, 69.6, 15.5 and 46.4 mg, respectively)

Compound **9** were isolated from Fr. 6-4 and Fr. 7-4 (13.2 mg in total)

Compound **11** was isolated from Fr. 6-1, Fr.6-4 and Fr. 7-4. (11.6 mg)

Isolation of known compounds from B. formasana leaf EtOH extract under dark circumstance

Compound **3**, **13**–**15**, **25** and **29** were isolated from Fr. 2-2 (2.3, 7.0, 61.5, 1.8, 51.8 and 8.4 mg).

Compound **26**, **27** and **32** were isolated from Fr.3-4 (4.9 mg and 7.4 mg, respectively)

Compound **30** was isolated from Fr.3-3 (13.6 mg)

Compound **31** was isolated from Fr.3-5 (8.8 mg)

Physiochemical data of the new compounds

8-(4″-Methoxyphenyl)-7-(3′,4′-dimethoxyphenyl)-1,2,3-dihydroindolizin-13-ium trifluoroacetate (1)

White amorphous solid; UV λ_{max} (MeOH) nm (log ε): 265 (4.45); IR (KBr): 3431, 1690, 1258, 1201, 1125, 1124 cm^{-1}; ^{1}H NMR and ^{13}C NMR data: see Table 1.; ESIMS $^{+}$ *m/z* 362.2 $[M]^{+}$; HR-ESIMS $^{+}$ *m/z* 362.1751 $[M]^{+}$; $C_{23}H_{24}NO_3$.

(4*S*, 6*S*, 7*R*, 9*S*)-6-(4′-Methoxyphenyl)-7-(3′,4′-dimethoxyphenyl)octahydro-indolizine-4-oxide (2)

Yellow solid; $[\alpha]_D^{25}$ −18.0 (*c* 0.1, MeOH); UV λ_{max} (MeOH) nm (log ε): 265 (4.45); CD (MeOH): $[\theta]_{279}$ -330; IR (KBr): 3479, 2951, 1964, 1516, 1435, 1205, 1144 cm^{-1}; ^{1}H NMR and ^{13}C NMR data: see Table 1.; ESIMS $^{+}$ *m/z* 384.2 $[M]^{+}$; HR-ESIMS $^{+}$ *m/z* 384.2169 $[M]^{+}$; $C_{23}H_{29}NO_4$.

(13a*S*,14*S*)-14-Hydroxy-2,3,6-trimethoxy-9-hydroantofinium TFA salt (6)

Yellow solid; $[\alpha]_D^{25}$ +5.8 (*c* 0.1, MeOH); UV λ_{max} (MeOH) nm (log ε): 265 (3.61); CD (MeOH): $[\theta]_{212}$ -1080; IR (KBr): 1682, 1210, 1139 cm^{-1}; ^{1}H NMR and ^{13}C NMR data: see Table 3.; ESIMS $^{+}$ *m/z* 378.0 $[M]^{+}$; HR-ESIMS $^{+}$ *m/z* 378.2 $[M]^{+}$; $C_{23}H_{24}NO_4$.

3,6-Dimethoxy-4a,4b-*seco*-phenanthroindolizidine (*seco*-Formonsanasine A) (7)

Yellow sold; UV λ_{max} (MeOH) nm (log ε): 275.0 (3.88); IR (KBr): 1693, 1649, 1518, 1506, 1463, 1292, 1254, 1181, 1126 cm^{-1}; ^{1}H NMR and ^{13}C NMR data, see Table 2.; ESIMS $^{+}$ *m/z* 332.1 $[M]^{+}$; HR-ESIMS $^{+}$ *m/z* 332.1676 $[M]^{+}$; $C_{22}H_{22}NO_2$.

4′-Methoxy-4″-hydroxy-6′,6″-*seco*-phenanthroindolizidine (*seco*-Formonsanasine B) (8)

Yellow solid; UV (MeOH): λ_{max} (log ε) 274.0 (3.73) nm; IR (KBr): 3212, 1689, 1608, 1543, 1488, 1208, 1134, 1026 cm^{-1}; ^{1}H NMR and ^{13}C NMR data: see Table 2.; ESIMS $^{+}$ *m/z* 318.1 $[M]^{+}$; HR-ESIMS $^{+}$ *m/z* 318.1515 $[M]^{+}$; $C_{21}H_{20}NO_2$.

3,5,6-Trimethoxy-11,12,13-trihyrodi-benzo[f,h]pyrrolo[1,2-b]isoquinoline (Tylophoridicine G) (10)

Yellow powder; UV (MeOH): λ_{max} (log ε) 213.0 (4.53) nm, 260.0 (4.29) nm and 279.0 (4.11) nm; IR (KBr): 2927, 1682, 1608, 1516, 1207, 1137 cm^{-1}; ^{1}H NMR data, see Table 2.; ESIMS $^{+}$ *m/z* 360.2 $[M]^{+}$; HR-ESIMS $^{+}$ *m/z* 360.1623 $[M]^{+}$; $C_{23}H_{22}NO_3$.

6-(4-Methoxyphenyl)-8-(4-hydroxyphenyl)-1,2,3-trihydroindolizidinium TFA salt (16)

White amorphous solid; UV λ_{max} (MeOH) nm (log ε): 268 (4.19), 339 (3.98); IR (KBr): 3797, 3545, 1653, 1507 cm^{-1}; ^{1}H NMR and ^{13}C NMR data, see Table 4.; ESIMS $^{+}$ *m/z* 318.1 $[M]^{+}$; HR-ESIMS $^{+}$ *m/z* 318.1489 $[M]^{+}$; $C_{21}H_{20}NO_2$.

6,8-*bis*(4,4-Hydroxyphenyl)-1,2,3-trihydroindolizidinium acetate (17)

White solid; UV λ_{max} (MeOH) nm (log ε): 266 (3.44); IR (KBr): 3390.6, 1747.5, 1204.7, 1134.4 cm^{-1}; ^{1}H NMR and ^{13}C NMR data, see Table 4.; ESIMS $^{+}$ *m/z* 304.1 $[M+59]^{+}$; $C_{20}H_{18}NO_2$.

6-(4-Methoxyphenyl)-8-(4,5-dimethoxyphenyl)-1,2,3-trihydroindolizidinium TFA salt (18)

White amorphous solid; UV λ_{max} (MeOH) nm (log ε): 266 (3.49); IR (KBr): 3445.0, 1682.4, 1519.0, 1207.4, 1133.7 cm^{-1}; ^1H NMR and ^{13}C NMR data, see Table 4.; ESIMS $^+$ *m/z* 362.2 $[M]^+$; HR-ESIMS $^+$ *m/z* 362.1745 $[M]^+$; $C_{23}H_{24}NO_3$.

6-(4,5-Dimethoxyphenyl)-8-(4-methoxyphenyl)-1,2,3-trihydroindolizidinium TFA salt (19)

White solid; UV λ_{max} (MeOH) nm (log ε): 266 (3.49); IR (KBr): 3390.5, 1747.5, 1204.7, 1134.4 cm^{-1}; ^1H NMR and ^{13}C NMR data, see Table 4.; ESIMS $^+$ *m/z* 362.2 $[M]^+$; HR-ESIMS $^+$ *m/z* 362.1759 $[M]^+$; $C_{23}H_{24}NO_3$.

Physiochemical data of known compounds

4a,4b-*seco*-Tetradehydroantofinium TFA salt (3)

Brown solid; ^1H NMR (400 MHz, CD_3OD): δ 8.82 (s, H-9), 8.03 (s, H-14), 7.17 (2H, d, J = 8.7 Hz, H-8/4b), 7.00 (1H, dd, J = 8.4, 1.6 Hz, H-4a), 6.99 (1H, d, J = 8.4 Hz, H-4), 6.95 (2H, d, J = 8.7 Hz, H-5/7), 6.72 (1H, d, J = 1.4 Hz, H-1), 4.85 (1H, t, J = 7.6 Hz, H-11), 3.83 (s, 6-OCH_3), 3.79 (s, 3-OCH_3), 3.57 (1H, t, J = 7.6 Hz, H-13), 3.53 (s, 2-OCH_3), 2.56 (1H, quin, J = 7.6 Hz, H-12); ^{13}C NMR (100 MHz, CD_3OD): δ 160.8 (C, C-6), 157.0 (C, C-14a), 156.7 (C, C-13a), 151.3 (C, C-3), 149.3 (C, C-2), 141.0 (CH, H-9), 138.1 (C, C-8b), 131.0 (CH, C-8/4b), 128.5 (C, C-14b), 127.1 (C, C-8a), 124.5 (CH, C-14), 123.1 (CH, C-4a), 114.5 (CH,C-5/7), 113.2 (CH, C-1), 111.7 (CH, C-4), 58.7 (CH_2, C-11), 55.4 (3-OCH_3), 55.2 (2-OCH_3), 54.9 (6-OCH_3), 31.9 (CH_2, C-13), 21.7 (CH_2, C-12); ESIMS $^+$ *m/z* 362.1 $[M]^+$.

Ficuseptine (4)

Light yellow solid; ^1H NMR (200 MHz, CD_3OD): δ 9.13 (1H, s, H-9), 8.60 (1H, s, H-14a), 7.78 (2H, d, J = 8.9 Hz, H-4b/8), 7.58 (2H, d, J = 8.9 Hz, H-1/4a), 7.14 (2H, d, J = 8.9 Hz, H-2/4), 7.12 (2H, d, J = 8.9 Hz, H-5/7), 4.97 (1H, t, J = 8.0 Hz, H-11), 3.87 (s, 3-OCH_3), 3.86 (s, 6-OCH_3), 3.57 (1H, t, J = 7.1 Hz, H-13), 2.52 (quin, J = 7.1 Hz, H-12); ESIMS $^+$ *m/z* 333.2 $[M + H]^+$.

4a,4b-*seco*-Dehydroantofine (5)

Light yellow solid; ^1H NMR (400 MHz, CD_3OD): δ 8.81 (1H, s, H-9), 8.03 (1H, s, H-14), 7.17 (2H, d, J = 8.8 Hz, H-8/4b), 7.00 (1H, dd, J = 8.6, 1.6 Hz, H-4a), 6.97 (1H, d, J = 8.6 Hz, H-4), 6.94 (2H, d, J = 8.8 Hz, H-5/7), 6.72 (1H, d, J = 1.6 Hz, H-1), 4.86 (1H, t, J = 7.6 Hz, H-11), 3.83 (s, 6-OCH_3), 3.79 (s, 3-OCH_3), 3.58 (1H, t, J = 7.6 Hz, H-13), 3.52 (s, 2-OCH_3), 2.57 (1H, quin, J = 7.6 Hz, H-12); ^{13}C NMR (100 MHz, CD_3OD): δ 160.8 (C, C-6), 157.0 (C, C-14a), 156.7 (C, C-13a), 151.3 (C, C-3), 149.3 (C, C-2), 141.0 (CH, C-9), 131.0 (CH, C-4b), 138.1 (C, C-8b), 131.0 (CH, C-8), 128.5 (C, C-14b), 127.1 (C, C-8a), 124.5 (CH, C-14), 123.1 (CH, C-4a), 114.5 (CH, C-5), 114.5 (CH, C-7), 113.2 (CH, C-1), 111.7 (CH, C-4), 58.7 (CH_2, C-11), 55.4 (3-OMe), 55.2 (2-OCH_3), 54.9 (6-OCH_3), 31.9 (CH_2, C-13), 21.7 (CH_2, C-12); ESIMS $^+$ *m/z* 364.0 $[M + H]^+$.

2,3,6-Trimethoxy-11,12,13,13a,14-pentahydrodibenzio[f,h]pyrrolo[1,2-b]isoquinoline (9)

Yellow liquid; $[\alpha]_D^{25}$ −20.0 (*c* 0.01, MeOH); UV (MeOH): λ_{max} (log ε) 415.0 (4.37) nm; IR (KBr) ν_{max}: 1682, 1613, 1519, 1207, 1133 cm^{-1}; ^1H NMR (400 MHz, CD_3OD): δ 9.84 (1H, s, H-9), 8.25 (1H, d, J = 9.4 Hz, H-8), 8.09 (1H, s, H-4), 8.06 (1H, d, J = 2.1 Hz, H-5), 7.59 (1H, s, H-1), 7.39 (1H, dd, J = 9.4, 2.1 Hz, H-7), 4.50 (1H, m, H-11), 4.31 (1H, m, H-13a), 4.30 (1H, m, H-11), 4.15 (1H, m, H-14), 4.10 (s, 2-OCH_3), 4.04 (s, 3-OCH_3), 4.04 (s, 6-OCH_3), 3.18 (1H, t, H-14), 2.70 (1H, quin, H-13), 2.40 (1H, quin, H-12), 2.20 (1H, m, H-12), 2.10 (1H, m, H-13); ^{13}C NMR (100 MHz, CD_3OD): δ 161.6 (CH, C-9), 160.7 (C, C-6), 155.2 (C, C-3), 155.1 (C, C-2), 125.2 (CH, C-8), 119.1 (CH, C-7), 107.1 (CH, C-1), 105.7 (CH, C-5), 105.4 (CH, C-4), 61.0 (CH, C-13a), 56.8 (2-OCH_3), 56.6 (6-OCH_3), 56.2 (3-OCH_3), 56.0 (CH_2, C-11), 32.6 (CH_2, C-13), 30.2 (CH, C-14), 24.2 (CH_2, C-12); ESIMS $^+$ *m/z* 362.1 $[M]^+$; HR-ESIMS $^+$ *m/z* 362.1745 $[M]^+$; $C_{23}H_{24}NO_3$.

Tylophoridicine D (11)

Yellow solid; ^1H NMR (400 MHz, CD_3OD): δ 10.02 (1H, s, H-9), 8.91 (1H, s, H-14), 8.70 (1H, d, J = 8.9 Hz, H-1), 7.99 (1H, s, H-8), 7.80 (1H, d, J = 2.2 Hz, H-4), 7.80 (1H, s, H-5), 7.34 (1H, dd, J = 8.9, 2.2 Hz, H-2), 4.98 (2H, t, H-11), 4.11 (s, 3-OCH_3), 4.09 (s, 6-OCH_3), 4.04 (s, 7-OCH_3), 3.65 (2H, t, H-13), 2.65 (2H, quin, H-12); ^{13}C NMR (100 MHz, CD_3OD): δ 162.5 (C, C-3), 155.0 (C, C-13a), 152.0 (C, C-6), 151.9 (C, C-7), 140.6 (CH, C-9), 138.6 (CH, C-1), 117.7 (CH, C-2), 117.6 (CH, C-14), 107.5 (CH, C-4), 107.2 (C, C-5), 106.1 (CH, C-8), 59.7 (CH_2, C-11), 56.9 (3-OCH_3), 56.8 (7-OCH_3), 56.3 (6-OCH_3), 32.5 (CH_2, C-13), 23.2 (CH_2, C-12); ESIMS $^+$ *m/z* 360.2 $[M]^+$.

Deoxytylophorinine (12)

Light yellow liquid; ^1H NMR (400 MHz, CD_3OD): δ 8.06 (1H, s, H-5), 8.00 (1H, d, J = 2.2 Hz, H-4), 7.80 (1H, d, J = 8.9 Hz, H-1), 7.38 (1H, s, H-8), 7.28 (1H, dd, J = 8.9, 2.2 Hz, H-4), 4.25 (1H, d, J = 16.0 Hz, H-9), 3.78 (1H, m H-14), 3.61 (1H, d, J = 16.0 Hz, H-9), 3.46 (1H, m, H-13a), 3.45 (1H, m, H-10), 3.25 (1H, m, H-10), 2.67 (1H, m, H-13), 2.30 (1H, m, H-12), 2.00 (1H, m, H-13); ESIMS $^+$ *m/z* 364.2 $[M + H]^+$.

(+)-Antofine (13)

Light yellow liquid; ^1H NMR (400 MHz, CD_3OD): δ 8.03 (1H, s, H-4), 8.00 (1H, d, J = 2.4 Hz, H-5), 7.80 (1H, d, J = 9.0 Hz, H-8), 7.35 (1H, s, H-1), 7.23 (1H, dd, J = 9.0, 2.4 Hz, H-1), 4.32 (1H, d, J = 14.8 Hz, H-

9), 4.07 (s, 2-OCH_3), 4.02 (s, 3-OCH_3), 4.01 (s, 6-OCH_3), 3.61 (1H, d, J = 14.7 Hz, H-9a), 2.52 (1H, m, H-13), 2.19 (1H, m, H-13), 1.96 (3H, m, H-12); ^{13}C NMR (100 MHz, CD_3OD): δ 157.6 (C, C-6), 149.6 (C, C-3), 148.3 (C, C-2), 130.4 (C, C-8a), 127.0 (C, C-4b), 126.2 (C, C-8b), 125.4 (C, C-15), 124.2 (CH, C-8), 124.0 (C, C-4a), 123.5 (C, C-15a), 114.8 (C, C-7), 104.6 (CH, C-5), 103.8 (CH, C-1), 103.7 (CH, C-4), 60.4 (C, C-13a), 56.0 (2-OCH_3), 55.8 (3-OCH_3), 55.5 (6-OCH_3), 54.9 (CH_2, C-11), 53.6 (CH_2, C-9), 33.4 (CH_2, C-14), 31.1 (CH_2, C-13), 21.5 (CH_2, C-12); ESIMS $^+$ m/z 364.0 $[M + H]^+$.

Tetradehydroantofinium TFA salt (14)

Yellow solid; ^{1}H NMR (400 MHz, CD_3OD): δ 9.83 (1H, s, 9-H), 8.66 (1H, s. H-14), 8.35 (1H, d, J = 9.0 Hz, H-8), 7.70 (1H, s, H-1), 7.41 (1H, d, J = 2.2 Hz, H-5), 7.39 (1H, s, H-4), 7.22 (1H, dd, J = 8.9, 2.2 Hz, H-7), 4.91 (1H, t, J = 7.6 Hz, H-11), 4.03 (s, 2-OCH_3), 4.02 (s, 3-OCH_3), 3.98 (s, 6-OCH_3), 3.59 (1H, t, J = 7.5 Hz, H-13), 2.64 (1H, quin, J = 7.5 Hz, H-12); ^{13}C NMR (100 MHz, CD_3OD): δ 161.7 (C, C-6), 154.1 (C, C-3), 151.1 (C, C-2), 151.3 (C, C-13a), 139.5 (C, C-14a), 137.7 (CH, C-9), 132.1 (C, C-4b), 128.4 (C, C-4a), 125.7 (CH, C-8), 125.6 (C, C-8b), 120.8 (C, C-14b), 119.6 (C, C-8a), 117.2 (CH, C-14), 117.1 (CH, C-7), 106.7 (CH, C-1), 106.5 (CH, C-5), 105.2 (CH, C-4), 59.6 (CH_2, C-11), 56.5 (2-OCH_3), 56.4 (3-OCH_3), 55.9 (6-OCH_3), 32.3 (CH_2, C-13), 23.0 (CH_2, C-12); ESIMS $^+$ m/z 360.1 $[M]^+$.

6,8-*bis*(4-Methoxyphenyl)-1,2,3-trihydroindolizidinium TFA salt (15)

White amorphous solid; ^{1}H NMR (400 MHz, CD_3OD): δ 9.12 (1H, s, H-5), 8.57 (1H, s, H-7), 7.77 (2H, d, J = 8.7 Hz, H-2′/6′), 7.57 (2H, d, J = 8.7 Hz, H-2″/6″), 7.11 (2H, d, J = 8.6 Hz, H-3′/5′), 7.10 (2H, d, J = 8.6 Hz, H-3″/5″), 4.96 (1H, t, J = 7.6 Hz, H-3), 3.85 (s, 4′-OCH_3), 3.85 (s, 4″-OCH_3), 3.55 (1H, t, J = 3.4 Hz, H-1), 2.51 (1H, quin, J = 7.4 Hz, H-2); ^{13}C NMR (100 MHz, CD_3OD): δ 162.9 (C, C-4′), 162.5 (C, C-4″), 155.6 (C, C-9), 142.3 (CH, C-7), 140.5 (C, C-6), 139.9 (C, C-8), 137.6 (CH, C-5), 131.2 (CH, C-2″/6″), 129.8 (CH, C-2′/6′), 128.1 (C, C-1″), 127.0 (C, C-1′), 116.1 (CH, C-3″/5″), 115.7 (CH, C-3′/5′), 61.1 (CH_2, C-3), 56.0 (4′-OCH_3), 56.0 (4″-OCH_3), 33.4 (CH_2, C-1), 22.9 (CH_2, C-2); ESIMS $^+$ m/z 332.1 $[M]^+$.

(*E*)-*O*-Methylferuloylagmatine (25)

Yellow liquid; ^{1}H NMR (400 MHz, CD_3OD): δ 7.45 (1H, d, J = 15.7 Hz, H-7), 7.14 (1H, d, J = 1.2 Hz, H-2), 7.11 (1H, dd, J = 8.4, 1.2 Hz, H-6), 6.95 (1H, d, J = 8.3 Hz, H-5), 6.49 (1H, d, J = 15.7 Hz, H-8), 3.85 (s, 3-OCH_3), 3.84 (s, 4-OCH_3), 3.33 (2H, br t, H-10), 3.22 (2H, br t, H-13), 1.63 (2H, br s, H-11), 1.63 (2H, br s, H-12); ^{13}C NMR (100 MHz, CD_3OD): δ 169.1 (C=O, C-9), 158.6 (C=N, C-14), 152.2 (C, C-4), 150.7 (C, C-3), 141.7 (CH, C-7), 129.3 (C, C-1), 123.2 (CH, C-6), 119.6 (CH, C-8), 112.7 (CH, C-5), 111.3 (CH, C-2), 56.4–56.5 (3/4-OCH_3), 42.1 (CH_2, C-13), 39.7 (CH_2, C-10), 27.8 (CH_2, C-12), 27.1 (CH_2, C-11); ESIMS $^+$ m/z 321.0 $[M+H]^+$.

(*E*)-1-(3-Methoxy-4-hydroxycinnamoyl)amino-13-guanidinobutane (26)

Transparent liquid; ^{1}H NMR (400 MHz, CD_3OD): δ 7.44 (1H, d, J = 15.7 Hz, H-7), 7.11 (1H, d, J = 1.7 Hz, H-2), 7.03 (1H, d, J = 8.1, 1.7 Hz, H-6), 6.79 (1H, d, J = 8.2 Hz, H-5), 6.42 (1H, d, J = 15.7 Hz, H-8), 3.88 (s, 3-OCH_3), 3.34 (overlapped by CD_3OD, H-10), 3.22 (1H, br t, H-13), 1.62 (1H, br t, H-11), 1.62 (1H, br t, H-12); ESIMS $^+$ m/z 307.1 $[M+H]^+$.

(*Z*)-1-(3,4-Dimethoxycinnamoyl)amino-13-guanidinobutane (27)

Transparent liquid; ^{1}H NMR (400 MHz, CD_3OD): δ 7.38 (1H, br s, H-2), 7.05 (1H, br d, J = 8.3 Hz, H-6), 6.89 (1H, d, J = 8.3 Hz, H-5), 6.66 (1H, d, J = 12.6 Hz, H-7), 5.89 (1H, d, J = 12.6 Hz, H-8), 3.83 (s, 5-OCH_3), 3.81 (s, 4-OCH_3), 3.25 (2H, br t, H-10), 3.17 (2H, br t, H-13), 1.56 (2H, br s, H-11), 1.56 (2H, br s, H-12), ^{13}C NMR (100 MHz, CD_3OD): δ 170.4 (C=O, C-9), 158.3 (C=N, C-14), 151.1 (C, C-4), 149.9 (C, C-3), 138.2 (CH, C-7), 129.8 (C, C-1), 124.6 (CH, C-6), 122.5 (CH, C-8), 114.2 (CH, C-2), 112.3 (CH, C-5), 56.4–56.5 (4/5-OCH_3), 42.1 (CH_2, C-13), 39.7 (CH_2, C-10), 27.2–27.5 (CH_2, C-11/12); ESIMS $^+$ m/z 321.2 $[M+H]^+$.

Boehmeriasine A (28)

White solid; ^{1}H NMR (400 MHz, $CDCl_3$): δ 7.90 (1H, d, J = 2.5 Hz, H-4), 7.90 (1H, s, H-5), 7.89 (1H, d, J = 9.0 Hz, H-1), 7.29 (1H, s, H-8), 7.21 (1H, dd, J = 9.0, 2.5 Hz, H-2), 4.69 (1H, d, J = 15.1 Hz, H-9), 4.10 (s, 3-OCH_3), 4.06 (s, 6-OCH_3), 4.01 (s, 7-OCH_3), 3.75 (1H, d, J = 15.1 Hz, H-9), 3.31 (dd, J = 16.0, 2.9 Hz, H-15), 2.30 (1H, m, H-11), 1.96 (1H, m, H-12), 1.96 (1H, m, H-13), 1.96 (1H, m, H-14); ESIMS $^+$ m/z 378.2 $[M + H]^+$.

Isopentyl *O*-β-glucopyranoside (29)

Transparent liquid; ^{1}H NMR (400 MHz, CD_3OD): δ 4.48 (1H, d, J = 7.9 Hz, H-1′), 3.99 (1H, m, H-1), 3.94 (1H, dd, J = 12.3, 2.0 Hz, H-6′), 3.75 (1H, m, H-6′), 3.72 (1H, m, H-1), 3.51 (1H, t, J = 9.2 Hz, H-3′), 3.46 (1H, m, H-5′), 3.40 (1H, m, H-4′), 3.28 (1H, t, J = 8.2 Hz, H-2′), 1.72 (1H, nonet, J = 6.8 Hz, H-3), 1.54 (2H, q, J = 7.9 Hz, H-2), 0.93 (6H, d, J = 6.7 Hz, H-4/5); ^{13}C NMR (100 MHz, CD_3OD): δ 103.2 (CH, C-1′), 76.9 (CH, C-3′), 76.8 (CH, C-5′), 74.1 (CH, C-2′), 70.6 (CH, C-4′), 70.1 (CH_2, C-1), 61.7 (CH_2, C-6′), 38.6 (CH_2, C-2), 25.2 (CH, C-3), 22.7 (CH_3, C-4/5); ESIMS $^+$ m/z 273.1 $[M+Na]^+$; ESIMS $^+$ m/z 523.1 $[2M + Na]^+$.

1-*O*-Benzyl β-glucopyranoside (30)

White liquid; ^{1}H NMR (400 MHz, CD_3OD): δ 7.40 (2H, br d, J = 7.6 Hz, H-2/6), 7.31 (2H, br t, J = 7.6 Hz,

H-3/5), 7.25 (1H, m, H-4), 4.91 (1H, dd, J = 11.7 Hz, H-7), 4.65 (1H, dd, J = 11.7 Hz, H-7), 4.34 (1H, d, J = 7.7 Hz, H-1′), 3.88 (1H, br d, J = 11.8 Hz, H-6′), 3.68 (1H, dd, J = 11.8, 5.6 Hz, H-6′), 3.22–3.44 (4H, m, H-2′-5′); ^{13}C NMR (100 MHz, CD_3OD): δ 139.1 (C, C-1), 129.2–129.3 (CH, C-2/3/5/6), 128.7 (CH, C-4), 103.1 (CH, C-1′), 78.1 (CH, C-3′), 78.0 (CH, C-5′), 75.1 (CH, C-2′), 71.7 (CH_2, C-7), 71.7 (CH, C-4′), 62.8 (CH_2, C-6′); ESIMS $^+$ m/z 293.1 $[M+Na]^+$.

1-*O*-Phenylethyl β-glucopyranoside (31)

Transparent liquid; ^{1}H NMR (400 MHz, CD_3OD): δ 7.43–7.38 (4H, m, H-2/3/5/6), 7.33 (1H, t, J = 8.1 Hz, H-4), 4.49 (1H, d, J = 7.9 Hz, H-1′), 4.18 (1H, m, H-8), 3.96 (1H, m, H-8), 3.91 (1H, br d, J = 12.2 Hz, H-6′), 3.73 (1H, dd, J = 12.2, 5.8 Hz, H-6′), 3.49 (1H, m, H-4′), 3.44 (1H, m, H-5′), 3.26 (1H, m, H-2′), 3.00 (1H, t, J = 6.8 Hz, H-7); ^{13}C NMR (100 MHz, CD_3OD): δ 139.7 (C, C-1), 130.0 (CH, C-2/3/5/6), 127.5 (CH, C-4), 103.2 (CH, C-1′), 76.9–76.8 (CH, C-3′/5′), 74.1 (CH, C-2′), 71.7 (CH_2, C-8), 70.6 (CH, C-4′), 61.7 (CH_2, C-6′), 36.2 (CH_2, C-7); ESIMS $^+$ m/z 307.1 $[M+Na]^+$.

5,7-Dihydroxychromone-7-*O*-β-glucopyranoside (32)

Brown solid; ^{1}H NMR (400 MHz, CD_3OD): δ 8.00 (1H, d, J = 5.9 Hz, H-2), 6.66 (1H, d, J = 1.8 Hz, H-8), 6.47 (1H, d, J = 1.8 Hz, H-6), 6.21 (1H, d, J = 5.9 Hz, H-3), 5.00 (1H, d, J = 7.0 Hz, H-1″), 3.87 (1H, dd, J = 12.1, 1.9 Hz, H-6″), 3.67 (1H, dd, J = 12.1, 5.6 Hz, H-6″), 3.30–3.50 (4H, m, H-2″-5″); ^{13}C NMR (100 MHz, CD_3OD): δ 183.6 (C=O, C-4), 164.3 (C, C-7), 163.4 (C, C-5), 159.5 (C, C-9), 158.6 (CH, C-2), 112.0 (CH, C-3), 108.4 (C, C-10), 101.6 (CH, C-1″), 101.3 (CH, C-6), 96.2 (CH, C-8), 78.4 (CH, C-5″), 77.9 (CH, C-3″), 74.7 (CH, C-2″), 71.2 (CH, C-4″), 62.4 (CH_2, C-6″); ESIMS $^+$ m/z 363.0 $[M + Na]^+$.

References

[1] Nho JW, Hwang IG, Kim HY, Lee YR, Woo KS, Hwang BY, et al. Free radical scavenging, angiotensin I-converting enzyme (ACE) inhibitory, and *in vitro* anticancer activities of Ramie (*Boehmeria nivea*) leaves extracts. Food Sci Biotechnol 2010;19:383–90.

[2] Chang JM, Huang KL, Yuan TTT, Lai YK, Hung LM. The anti-hepatitis B virus activity of *Boehmeria nivea* extract in HBV-Viremia SCID mice. Evid Based Complement Alternat Med 2010;7:189–95.

[3] Huang KL, Lai YK, Lin CC, Chang JM. Involvement of GRP78 in inhibition of HBV secretion by *Boehmeria nivea* extract in human HepG2 2.2.15 cells. J Viral Hepat 2009;16:367–75.

[4] Huang KL, Lai YK, Lin CC, Chang JM. Inhibition of hepatitis B virus production by Boehmeria nivea root extract in HepG2 2.2.15 Cells. World J Gastroenterol 2006;12:5721–5.

[5] Semwal DK, Rawat U, Semwal R, Singh R, Krishan P, Singh M, et al. Chemical constituents from the leaves of *Boehmeria rugulosa* with antidiabetic and antimicrobial activities. J Asian Nat Prod Res 2009;11:1045–55.

[6] Luo Y, Liu Y, Luo D, Gao X, Li B, Zhang G. Cytotoxic alkaloids from *Boehmeria siamensis*. Planta Med 2003;69:842–5.

[7] Min Y, Yang J, Ping Y, Liu W. Chemical constituents of *Boehmeria macrophylla* hornem. J Adv Mat Res 2012;550:1378–80.

[8] Matsuura S, Lee L, Iinuma M. Studies on the components of *Boehmeria sp. I.* Studies on the components of the roots of *Boehmeria platanifolia* Franch. et Sav (author's transl)]. Yakugaku Zasshi 1973;93:1682–4.

[9] Oyarzún ML, Garbarino JA, Gambaro V, Guilhem J. Two triterpenoids from *Boehmeria excelsa*. Phytochemistry 1986;26:221–3.

[10] Cai XF, Jin X, Lee D, Yang YT, Lee K. Phenanthroquinolizidine alkaloids from the roots of *Boehmeria pannosa* potently inhibit hypoxia-inducible factor-1 in AGS human gastric cancer cells. J Nat Prod 2006;69:1095–7.

[11] Al-Shamma A, Drake SD, Guagliardi LE, Mitscher LA. Antimicrobial alkaloids from *Boehmeria cylindrical*. Phytochemistry 1982;21:485–7.

[12] Takemoto T, Miyasi T, Kusano G. Flavones and other compounds of B*oehmeria tricuspis* and *B. holosericea*. Yakugaku Zasshi 1975;14:2534.

[13] Ngo DH, Ryu B, Vo TS, Himaya SWA. Free radical scavenging and angiotensin-I converting enzyme inhibitory peptides from pacific cod (*Gadus macrocephalus*) skin gelatin. Int J Biol Macromol 2011;49:1110–6.

[14] World Health Organization. Diabetes. Available at: https://www.who.int/health-topics/diabetes. [Accessed 15 July 2021].

[15] Mehanna AS. Insulin and oral antidiabetic agent. Am J Pharmaceut Educ 2005;69.

[16] Baggio LL, Drucker DJ. Biology of incretins: GLP-1 and GIP. Gastroenterology 2007;132:2131–57.

[17] Blundell JE, Naslund E. Glucagon-like peptide-1, satiety and appetite control. Br J Nutr 1999;81:259–60.

[18] Edholm T, Degerblad M, Gryback P. Differential incretin effects of GIP and GLP-1 on gastric emptying, appetite, and insulin-glucose homeostasis. Neuro Gastroenterol Motil 2010;22:1191–200.

[19] Appel SJ. Tapping incretin-based therapy for type 2 diabetes. Nursing 2011;41:49–51.

[20] Stoye A, Peez TE, Opatz T. Left, right, or both? On the configuration of the phenanthroindolizidine alkaloid tylophorine from *Tylophora indica*. J Nat Prod 2013;76:275–8.

[21] Govindachachari R, Viswanathan N. Recent progress in the chemistry of phenanthroindolizidine alkaloids. Heterocycles 1978;11:588–613.

[22] Othman WNNW, Sivasothy Y, Liew SY, Mohamad J, Nafiah MA, Ahmad K, et al. Alkaloids from *Cryptocarya densiflora* Blume (Lauraceae) and their cholinesterase inhibitory activity. Phytochem Lett 2017;21:230–6.

[23] Baumgartner B, Erdelmeier CAJ, Wright AD, Rali T, Sticher O. An antimicrobial alkaloid from *Ficus septica*. Phytochemistry 1990;29:3327–30.

[24] Wu TS, Su CR, Lee KH. Cytotoxic and anti-HIV phenanthroindolizidine alkaloids from *Cryptocarya chinensis*. Nat Prod Commun 2012;7:725–7.

[25] Jia XH, Zhao HX, Du CL, Tang WZ, Wang XJ. Possible pharmaceutical applications can be developed from naturally occurring phenanthroindolizidine and phenanthroquinolizidine alkaloids. Phytochemistry Rev 2020;20:845–68.

[26] Su CR, Damu AG, Chiang PC, Bastow KF, Morris-Natschke SL, Lee KH, et al. Total synthesis of phenanthroindolizidine alkaloids (±)-antofine, (±)-deoxypergularinine, and their dehydro congeners and evaluation of their cytotoxic activity. Bioorg Med Chem 2008;16:6233–41.

[27] Zhen YY, Huang XS, Yu DQ, Yu SS. Antitumor alkaloids isolated from *Tylophora ovata*. Acta Bot Sin 2002;44:349–53.

[28] Kubo M, Yatsuzuka W, Matsushima S, Harada K, Inoue Y, Miyamoto H, et al. Antimalarial phenanthroindolizine alkaloids from *Ficus septica*. Chem Pharm Bull 2016;64:957–60.